

f-Element/Crown Ether Complexes. 17.¹ Synthetic and Structural Survey of Lanthanide Chloride Triethylene Glycol Complexes

Robin D. Rogers,* Eric J. Voss, and Russell D. Etzenhouser

Received July 22, 1987

Triethylene glycol impurities in the reactions of the hydrated chloride salts of Dy and Y with 18-crown-6 in 1:3 solutions of methanol and acetonitrile saturated with LiCl yield the anhydrous crystalline $[\text{MCl}_3(\text{triethylene glycol})] \cdot 18\text{-crown-6}$ ($\text{M} = \text{Dy}, \text{Y}$). These isostructural complexes (monoclinic, space group $C2/c$) crystallize as polymeric chains of 18-crown-6 molecules, residing around crystallographic centers of inversion, hydrogen-bonded to pentagonal-bipyramidal $[\text{MCl}_3(\text{triethylene glycol})]$ moieties (which reside on crystallographic 2-fold axes). Cell data for these complexes are as follows: $\text{M} = \text{Dy}$ (-150°C), $a = 16.361$ (5) Å, $b = 13.620$ (1) Å, $c = 11.889$ (3) Å, $\beta = 92.28$ (2)°, and $D_{\text{calcd}} = 1.71 \text{ g cm}^{-3}$ for $Z = 4$; $\text{M} = \text{Y}$ (-150°C), $a = 16.352$ (4) Å, $b = 13.600$ (5) Å, $c = 11.890$ (3) Å, $\beta = 92.54$ (2)°, and $D_{\text{calcd}} = 1.53 \text{ g cm}^{-3}$ for $Z = 4$; $\text{M} = \text{Y}$ (20°C), $a = 16.606$ (5) Å, $b = 13.786$ (4) Å, $c = 11.830$ (5) Å, $\beta = 92.42$ (3)°, and $D_{\text{calcd}} = 1.50 \text{ g cm}^{-3}$ for $Z = 4$. The reactions of pure triethylene glycol with hydrated lanthanide salts in the same solvent mixture have also been investigated. Most of the early lanthanides (La, Ce, Sm) have yielded only viscous oils from which we have been unable to obtain single crystals. For the early lanthanide Nd and mid-series lanthanides Eu, Gd, and Dy (and the similar Y), nine-coordinate hydrated salts, $[\text{M}(\text{OH}_2)_9(\text{triethylene glycol})]\text{Cl}_3$, have been isolated and structurally characterized. These complexes are isostructural (orthorhombic, $Pna2_1$), crystallizing in a complex hydrogen-bonding network connecting the chloride ions to the tricapped-trigonal-prismatic $[\text{M}(\text{OH}_2)_9(\text{triethylene glycol})]^{3+}$ ions. Cell data for these complexes are as follows: $\text{M} = \text{Nd}$ (20°C), $a = 14.463$ (2) Å, $b = 9.746$ (1) Å, $c = 12.224$ (1) Å, and $D_{\text{calcd}} = 1.89 \text{ g cm}^{-3}$ for $Z = 4$; $\text{M} = \text{Eu}$ (-150°C), $a = 14.330$ (2) Å, $b = 9.679$ (1) Å, $c = 12.107$ (1) Å, and $D_{\text{calcd}} = 1.97 \text{ g cm}^{-3}$ for $Z = 4$; $\text{M} = \text{Gd}$ (20°C), $a = 14.344$ (1) Å, $b = 9.708$ (1) Å, $c = 12.154$ (2) Å, and $D_{\text{calcd}} = 1.98 \text{ g cm}^{-3}$ for $Z = 4$; $\text{M} = \text{Dy}$ (20°C), $a = 14.282$ (2) Å, $b = 9.687$ (1) Å, $c = 12.121$ (1) Å, and $D_{\text{calcd}} = 2.02 \text{ g cm}^{-3}$ for $Z = 4$; $\text{M} = \text{Y}$ (20°C), $a = 14.256$ (2) Å, $b = 9.675$ (1) Å, $c = 12.104$ (1) Å, and $D_{\text{calcd}} = 1.73 \text{ g cm}^{-3}$ for $Z = 4$. The formation of the $\text{M} = \text{Sm}$ complex has been confirmed by elemental analysis. The later lanthanides are more difficult to crystallize. Two of these complexes, $\text{M} = \text{Ho}$ and Lu , have been obtained as anhydrous acetonitrile solvates, $[\text{MCl}_3(\text{triethylene glycol})] \cdot \text{CH}_3\text{CN}$. These two complexes are isostructural (monoclinic, $P2_1/c$) and exist in a pentagonal-bipyramidal geometry participating in a complex hydrogen-bonded network in which the alcoholic and solvent methyl hydrogen atoms donate to the two axial coordinated chloride atoms in symmetry-related units. Cell data for these complexes are as follows: $\text{M} = \text{Ho}$ (20°C), $a = 9.048$ (2) Å, $b = 10.904$ (1) Å, $c = 16.434$ (2) Å, $\beta = 103.96$ (2)°, and $D_{\text{calcd}} = 1.95 \text{ g cm}^{-3}$ for $Z = 4$; $\text{M} = \text{Lu}$ (20°C), $a = 8.999$ (2) Å, $b = 10.792$ (5) Å, $c = 16.338$ (3) Å, $\beta = 103.80$ (2)°, and $D_{\text{calcd}} = 2.04 \text{ g cm}^{-3}$ for $Z = 4$. Complexes with $\text{M} = \text{Er}$ and Yb have been isolated as isostructural (monoclinic, $P2_1/c$) methanol solvates, $[\text{MCl}_3(\text{triethylene glycol})] \cdot \text{OHMe}$, and have the same coordination geometry as for $\text{M} = \text{Ho}$ and Lu in the acetonitrile solvates. Cell data are as follows: $\text{M} = \text{Er}$ (20°C), $a = 7.460$ (2) Å, $b = 14.402$ (5) Å, $c = 14.220$ (2) Å, $\beta = 101.93$ (2)°, and $D_{\text{calcd}} = 2.02 \text{ g cm}^{-3}$ for $Z = 4$; $\text{M} = \text{Yb}$ (20°C), $a = 7.440$ (1) Å, $b = 14.350$ (4) Å, $c = 14.214$ (4) Å, $\beta = 102.10$ (2)°, and $D_{\text{calcd}} = 2.07 \text{ g cm}^{-3}$ for $Z = 4$. $\text{M} = \text{Lu}$ has been confirmed by preliminary unit cell determination. The hydrogen bonding results in parallel polymeric chains. Formula units in the chains are bridged by hydrogen bonding to and from the methanol molecules. The chains are bridged by complementary alcoholic hydrogen to axial chlorine (and vice versa) hydrogen bonds. The anhydrous and solvent-free $[\text{LuCl}_3(\text{triethylene glycol})]$ has also been structurally characterized. This complex crystallizes in the orthorhombic space group $Pbcn$ with $a = 7.5893$ (6) Å, $b = 11.130$ (1) Å, $c = 14.802$ (2) Å, and $D_{\text{calcd}} = 2.29 \text{ g cm}^{-3}$ for $Z = 4$. The Lu atom resides on a crystallographic 2-fold axis with a geometry similar to that of all of the structurally characterized seven-coordinate species of this type. The hydrogen bonding to axial chlorines produces zigzag polymeric chains along c .

Introduction

We have begun carrying out systematic investigations of the structural chemistry of f-element/crown ether complexes.¹ We originally entered this area as a route to novel organo-f-element chemistry and have thus concentrated on hydrated chloride salts of the f metals¹⁻⁹ and methods of easily preparing anhydrous crown ether chloride complexes. Some of the more interesting results have been obtained by utilizing 18-crown-6 (which has a cavity size best suited for the early Ln(III) ions) and mid- to late-lanthanide chloride salts. Among the 18-crown-6 complexes that we have structurally characterized are $[\text{MCl}(\text{OH}_2)_2(18\text{-crown-6})]\text{Cl}_2 \cdot 2\text{H}_2\text{O}$ ($\text{M} = \text{Sm}, \text{Gd}, \text{Tb}$),⁸ $[\text{M}(\text{OH}_2)_7(\text{OHMe})][\text{MCl}(\text{OH}_2)_2(18\text{-crown-6})_2]\text{Cl}_2 \cdot 2\text{H}_2\text{O}$ ($\text{M} = \text{Dy}, \text{Y}$),⁹ and $[\text{Dy}(\text{OH}_2)_8]\text{Cl}_3 \cdot 18\text{-crown-6} \cdot 4\text{H}_2\text{O}$.¹

None of the 18-crown-6 complexes we had thus far prepared had been anhydrous; a varying number of water molecules had always been retained, stabilizing the structure via coordination to the metal, hydrogen bonding to the chloride ions, or both. While investigating the use of LiCl to increase chloride ion concentration

in our reactions, we happened to isolate anhydrous triethylene glycol complexes resulting from the use of an impure sample of 18-crown-6. (In some industrial processes, triethylene glycol is a starting material in reactions to form 18-crown-6.) These complexes, $[\text{MCl}_3(\text{triethylene glycol})] \cdot 18\text{-crown-6}$ ($\text{M} = \text{Dy}, \text{Y}$), piqued our interest in utilizing triethylene glycol itself as a route to anhydrous lanthanide chloride complexes.

A survey of two excellent reviews on crown ether chemistry^{10,11} and one on multidentate acyclic ligands¹² revealed the complexation chemistry of polyethylene glycols to be relatively unexplored, especially for the f elements. Those studies that had been carried out increased our interest in these complexes. First, the pseudocavity created by complexation of a polyethylene glycol can be tailored to fit the smaller lanthanide(III) ions by variation of ethylene units (as opposed to the rather constant cavity size of 18-crown-6). Second, the decomplexation of polyethylene glycols appears to be much easier than for corresponding crown ethers. (This fact could bode well for preparation of soluble anhydrous lanthanide chloride complexes and development of further organometallic chemistry.) Finally, polyethylene glycols have been hinted at as possible phase-transfer catalysts and separations agents.^{12,13}

(1) Part 16: Rogers, R. D. *Inorg. Chim. Acta* **1987**, *133*, 347.

(2) Rogers, R. D. *J. Coord. Chem., Sect. A*, in press.

(3) Rogers, R. D.; Voss, E. J. *Inorg. Chim. Acta* **1987**, *133*, 181.

(4) Rogers, R. D. *Inorg. Chim. Acta* **1987**, *133*, 175.

(5) Rogers, R. D.; Kurihara, L. K. *Inorg. Chim. Acta* **1987**, *129*, 277.

(6) Rogers, R. D.; Kurihara, L. K. *Inorg. Chim. Acta* **1987**, *130*, 131.

(7) Rogers, R. D.; Kurihara, L. K. *Inorg. Chim. Acta* **1986**, *116*, 171.

(8) Rogers, R. D.; Kurihara, L. K. *Inorg. Chem.* **1987**, *26*, 1498.

(9) Rogers, R. D.; Kurihara, L. K.; Voss, E. J. *Inorg. Chem.* **1987**, *26*, 2360.

(10) Bunzli, J.-C. G.; Wessner, D. *Coord. Chem. Rev.* **1984**, *60*, 191.

(11) Bunzli, J.-C. G. In *Handbook on the Physics and Chemistry of Rare Earths*; Gschneider, K. A., Jr., Eyring, L., Eds.; Elsevier: New Amsterdam, The Netherlands; in press.

(12) Vogtle, F.; Weber, E. *Angew. Chem., Int. Ed. Engl.* **1979**, *18*, 753.

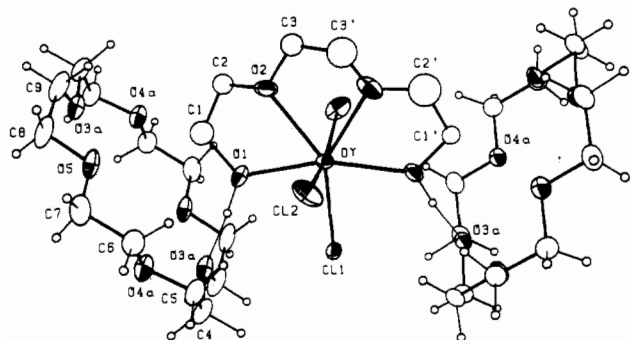


Figure 1. ORTEP illustration of a portion of one of the polymeric chains found in $[\text{MCl}_3(\text{EO}_3)] \cdot 18\text{-crown-6}$ ($\text{M} = \text{Dy}$ (shown), Y). The atoms are represented by their 50% probability thermal ellipsoids.

All of the above led us to the present study: a survey of the structural chemistry of lanthanide chloride triethylene glycol derivatives. This study was intended to further our understanding from a solid-state point of view of what factors such as coordination number, coordination geometry, metal size, and hydrogen bonding control complexation. In addition, as a result of triethylene glycol's flexibility and adaptability to a variety of coordination geometries, we felt that we would find more structural changes among the lanthanide series as the metal ion size decreased than would be observed with crown ethers.

Hirashima has published several accounts of polyethylene glycol derivatives of hydrated lanthanide nitrates¹³⁻¹⁸ and one of hydrated lanthanide chlorides.¹⁹ We will follow the abbreviations used for these glycols in these papers (e.g., triethylene glycol = EO3, tetraethylene glycol = EO4, etc.) A few structures of these glycols complexed with lanthanide nitrates have been reported, including $[\text{M}(\text{NO}_3)_3(\text{EO}_3)]$ ($\text{M} = \text{Nd},^{17} \text{Eu}^{20}$), $[\text{M}(\text{NO}_3)_3(\text{EO}_4)]$ ($\text{M} = \text{La},^{21} \text{Nd}^{15}$), and $[\text{Nd}(\text{NO}_3)_2(\text{EO}_5)][\text{NO}_3]$.¹⁶ Some work with alkali and alkaline-earth metals has also appeared,²² and the structures of $[\text{Ca}(\text{pcr})_2(\text{OH}_2)(\text{EO}_4)]^{23}$ (pcr = picrate) and $[\text{Sr}(\text{NCS})(\text{EO}_7)][\text{SCN}]^{24}$ have been reported.

Synthetic Results

The reaction of hydrated lanthanide chloride salts with triethylene glycol in a 1:1 molar ratio in a 1:3 mixture of acetonitrile and methanol has produced 1:1 triethylene glycol derivatives for all of the lanthanides studied (La, Ce, Nd, Sm-Er, Tb, Lu). Analytical and structural data have been used to confirm two different types of coordination complexes. The early- and mid-series lanthanides crystallizes as the nine-coordinate species $[\text{M}(\text{OH}_2)_5(\text{EO}_3)]\text{Cl}_3$. Crystal structures have been obtained for $\text{M} = \text{Nd}, \text{Eu}, \text{Gd}, \text{Dy}$, and Y . Analytical data only have been used to confirm the identical formula for $\text{M} = \text{Sm}$.

Late lanthanides crystallize as anhydrous seven-coordinate species. These can be acetonitrile solvates, $[\text{MCl}_3(\text{EO}_3)] \cdot \text{CH}_3\text{CN}$

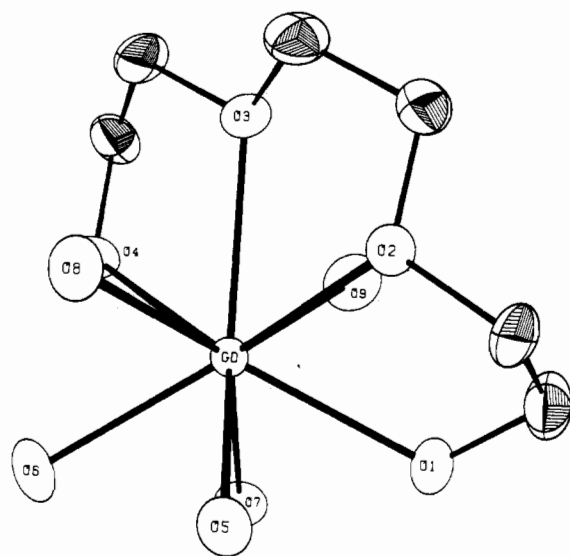


Figure 2. View down the pseudo-3-fold axis in the tricapped trigonal prism found for the $[\text{M}(\text{OH}_2)_5(\text{EO}_3)]^{3+}$ cations ($\text{M} = \text{Nd}, \text{Eu}, \text{Gd}$ (shown), Dy, Y).

($\text{M} = \text{Ho}, \text{Lu}$ have been structurally characterized), methanol solvates, $[\text{MCl}_3(\text{EO}_3)] \cdot \text{OHMe}$ ($\text{M} = \text{Er}, \text{Yb}$), or the unsolvated complex, $[\text{MCl}_3(\text{EO}_3)]$ ($\text{M} = \text{Lu}$). The acetonitrile solvates can be easily transformed to the pure complexes by removing the solvent from the crystals under vacuum.

The same seven-coordinate metal geometry has been obtained for $\text{M} = \text{Dy}$ and Y via the unintentional triethylene glycol impurities in the reaction of 18-crown-6 with hydrated chloride salts of these metals in the same solvent mixture as above that had been saturated with LiCl . These complexes are most similar to the solvates mentioned above, with 18-crown-6 acting as a hydrogen bond acceptor in the structures of $[\text{MCl}_3(\text{EO}_3)] \cdot 18\text{-crown-6}$.

Structural Results

$[\text{MCl}_3(\text{EO}_3)] \cdot 18\text{-crown-6}$ ($\text{M} = \text{Dy}, \text{Y}$). An ORTEP drawing depicting the polymeric nature of the hydrogen bonding in these complexes is presented in Figure 1; bond distances and angles for all three determinations of this complex type ($\text{M} = \text{Y}$ at 20 and -150°C) are given in the supplementary material. Coordination distances are averaged in the Discussion. Each metal ion is seven-coordinate with a distorted-pentagonal-bipyramidal geometry. The metal ion and equatorial chlorine atom ($\text{Cl}(1)$) reside on a crystallographic 2-fold axis. The four coordinated EO3 oxygen atoms reside in the pentagonal plane with $\text{Cl}(1)$. These atoms are planar to within 0.06 \AA (with $\text{M} = \text{Dy}$ as an example). The distortion occurs with the axial chlorine ligands. Each is displaced away from $\text{Cl}(1)$ toward $\text{C}(3)\text{-C}(3)'$. The $\text{Cl}(2)\text{-M-Cl}(2)^a$ angle is $163.96(8)^\circ$ for $\text{M} = \text{Dy}$.

The carbon atoms of the EO3 ligand are disordered, resulting in two different conformations of this moiety. The glycol hydrogen atoms are hydrogen-bonded to an 18-crown-6 molecule ($\text{O}(3)$), which accepts two such interactions from symmetry-related units. The 18-crown-6 molecule resides around a center of inversion and displays its full D_{3d} symmetry. The hydrogen bonding results in polymeric chains, as depicted in Figure 1, which propagate along the unit cell axis a . There is no interaction between chains and no hydrogen bonding to the chlorine atoms. For $\text{M} = \text{Dy}$, $\text{H}(1)\text{[O}(1)] \cdots \text{O}(3) = 1.604 \text{ \AA}$, $\text{O}(1)\text{-H}(1)\text{[O}(1)] \cdots \text{O}(3) = 174^\circ$, and $\text{O}(1) \cdots \text{O}(3) = 2.664(6) \text{ \AA}$. The 18-crown-6 molecule is ordered with average bonding parameters of $\text{C-O} = 1.428(4) \text{ \AA}$, $\text{C-C} = 1.50(1) \text{ \AA}$, $\text{C-C-O} = 108.5(5)^\circ$, and $\text{C-O-C} = 111.7(9)^\circ$ for $\text{M} = \text{Dy}$.

$[\text{M}(\text{OH}_2)_5(\text{EO}_3)]\text{Cl}_3$ ($\text{M} = \text{Nd}, \text{Eu}, \text{Gd}, \text{Dy}, \text{Y}$). Bond distances and angles for this series are presented in Table I. As depicted in Figure 2 for $\text{M} = \text{Gd}$, each metal ion is nine-coordinate, five coordination sites being occupied by water molecules and four by the EO3 ligand. There are no tight ion pairs in these structures. The tricapped-trigonal-prismatic metal coordination geometry is

- (13) Hirashima, Y.; Moriwaki, Y.; Shiokawa, J. *Chem. Lett.* **1980**, 1181.
- (14) Hirashima, Y.; Shiokawa, J. *Chem. Lett.* **1979**, 463.
- (15) Hirashima, Y.; Tsutsui, T.; Shiokawa, J. *Chem. Lett.* **1981**, 1501.
- (16) Hirashima, Y.; Kanetsuki, K.; Shiokawa, J.; Tanaka, N. *Bull. Chem. Soc. Jpn.* **1981**, *54*, 1567.
- (17) Hirashima, Y.; Tsutsui, T.; Shiokawa, J. *Chem. Lett.* **1982**, 1405.
- (18) Hirashima, Y.; Kanetsuki, K.; Yonezu, I.; Kamakura, K.; Shiokawa, J. *Bull. Chem. Soc. Jpn.* **1983**, *56*, 738.
- (19) Hirashima, Y.; Ito, K.; Shiokawa, J. *Chem. Lett.* **1983**, 9.
- (20) Forsellini, E.; Casellato, U.; Tomat, G.; Graziani, R.; Di Bernardo, P. *Acta Crystallogr., Sect. C: Cryst. Struct. Commun.* **1984**, *C40*, 795.
- (21) Casellato, U.; Tomat, G.; Di Bernardo, P.; Graziani, R. *Inorg. Chim. Acta* **1982**, *61*, 181.
- (22) Sieger, H.; Vogtle, F. *Tetrahedron Lett.* **1978**, *30*, 2709.
- (23) Singh, T. P.; Reinhardt, R.; Poonia, N. S. *Inorg. Nucl. Chem. Lett.* **1980**, *16*, 293.
- (24) Ohmoto, H.; Kai, Y.; Yasuoka, N.; Kasai, N.; Yanagida, S.; Okahara, M. *Bull. Chem. Soc. Jpn.* **1979**, *52*, 1209.
- (25) Shannon, R. D. *Acta Crystallogr., Sect. A: Cryst. Phys., Diffraction, Theor. Gen. Crystallogr.* **1976**, *A32*, 751.
- (26) SHELX, a system of computer programs for X-ray structure determination by G. M. Sheldrick, as locally modified (1976).
- (27) *International Tables for X-ray Crystallography*; Kynoch: Birmingham, England, 1972; Vol. IV.

Table I. Bond Distances (Å) and Angles (deg) for $[M(OH_2)_5(EO_3)]Cl_3$

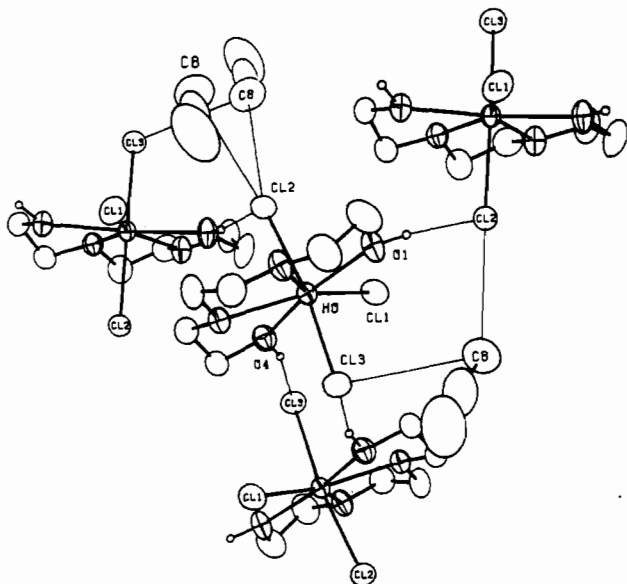
atoms	M = Nd	M = Eu	M = Gd	M = Dy	M = Y
M-O(1)	2.480 (7)	2.457 (7)	2.440 (5)	2.416 (6)	2.420 (5)
M-O(2)	2.500 (8)	2.471 (9)	2.466 (7)	2.445 (7)	2.439 (6)
M-O(3)	2.596 (7)	2.577 (7)	2.564 (6)	2.539 (6)	2.544 (6)
M-O(4)	2.469 (7)	2.426 (7)	2.408 (5)	2.373 (6)	2.376 (6)
M-O(5)	2.497 (6)	2.451 (7)	2.451 (5)	2.423 (5)	2.413 (5)
M-O(6)	2.506 (7)	2.483 (8)	2.455 (6)	2.428 (6)	2.437 (6)
M-O(7)	2.496 (9)	2.453 (9)	2.447 (7)	2.413 (8)	2.406 (6)
M-O(8)	2.495 (7)	2.447 (8)	2.443 (6)	2.395 (6)	2.400 (6)
M-O(9)	2.514 (6)	2.455 (7)	2.463 (5)	2.421 (5)	2.418 (5)
O(1)-C(1)	1.45 (1)	1.44 (1)	1.44 (1)	1.43 (1)	1.42 (1)
O(2)-C(2)	1.47 (1)	1.45 (1)	1.46 (1)	1.45 (1)	1.46 (1)
O(2)-C(3)	1.43 (1)	1.44 (1)	1.41 (1)	1.44 (1)	1.44 (1)
O(3)-C(4)	1.44 (1)	1.45 (1)	1.44 (1)	1.45 (1)	1.45 (1)
O(3)-C(5)	1.45 (1)	1.41 (1)	1.45 (1)	1.42 (1)	1.44 (1)
O(4)-C(6)	1.43 (1)	1.42 (1)	1.46 (1)	1.44 (1)	1.42 (1)
C(1)-C(2)	1.45 (2)	1.49 (2)	1.47 (1)	1.48 (1)	1.48 (1)
C(3)-C(4)	1.43 (1)	1.49 (2)	1.48 (1)	1.47 (1)	1.47 (1)
C(5)-C(6)	1.46 (2)	1.50 (2)	1.47 (2)	1.53 (2)	1.51 (1)
O(1)-M-O(2)	64.7 (2)	65.4 (3)	65.6 (2)	65.7 (3)	65.9 (2)
O(1)-M-O(3)	113.9 (2)	114.5 (3)	114.1 (2)	115.0 (2)	114.7 (2)
O(2)-M-O(3)	62.1 (2)	63.4 (3)	62.5 (2)	63.2 (2)	63.0 (2)
O(1)-M-O(4)	148.7 (2)	146.9 (3)	147.6 (2)	147.1 (2)	147.2 (2)
O(2)-M-O(4)	125.3 (2)	126.7 (3)	126.7 (2)	127.9 (2)	126.8 (2)
O(3)-M-O(4)	63.5 (2)	63.6 (3)	64.6 (2)	64.9 (2)	64.1 (2)
O(1)-M-O(5)	69.6 (2)	69.9 (3)	69.5 (2)	69.1 (2)	69.2 (2)
O(2)-M-O(5)	78.8 (3)	78.0 (4)	78.4 (3)	78.5 (3)	78.5 (2)
O(3)-M-O(5)	130.2 (3)	131.1 (3)	131.0 (3)	131.6 (3)	131.2 (2)
O(4)-M-O(5)	137.9 (2)	138.6 (3)	138.0 (2)	137.9 (2)	137.9 (2)
O(1)-M-O(6)	122.4 (3)	123.1 (3)	122.1 (2)	121.8 (3)	121.8 (2)
O(2)-M-O(6)	143.9 (3)	143.3 (3)	142.7 (2)	142.6 (2)	142.8 (2)
O(3)-M-O(6)	123.6 (2)	122.4 (3)	123.8 (2)	123.2 (2)	123.5 (2)
O(4)-M-O(6)	69.2 (2)	68.3 (2)	68.8 (2)	68.3 (2)	68.8 (2)
O(5)-M-O(6)	72.8 (3)	73.6 (3)	72.5 (2)	72.3 (3)	72.3 (2)
O(1)-M-O(7)	71.7 (3)	71.1 (3)	71.1 (2)	71.9 (3)	70.9 (2)
O(2)-M-O(7)	135.5 (3)	135.9 (3)	136.0 (2)	136.9 (2)	136.0 (2)
O(3)-M-O(7)	134.6 (3)	134.8 (3)	134.6 (2)	134.2 (2)	133.9 (2)
O(4)-M-O(7)	88.5 (3)	87.6 (3)	87.5 (2)	85.5 (2)	87.1 (2)
O(5)-M-O(7)	94.8 (3)	93.8 (4)	94.0 (3)	93.9 (3)	94.5 (3)
O(6)-M-O(7)	69.8 (3)	69.4 (3)	69.8 (2)	69.1 (3)	69.8 (2)
O(1)-M-O(8)	129.5 (3)	129.9 (3)	129.7 (2)	129.7 (2)	129.3 (2)
O(2)-M-O(8)	78.3 (3)	76.7 (3)	77.0 (2)	76.8 (2)	76.6 (2)
O(3)-M-O(8)	72.0 (2)	71.6 (3)	72.2 (2)	72.2 (2)	72.5 (2)
O(4)-M-O(8)	80.9 (2)	82.3 (3)	82.0 (2)	82.7 (2)	82.9 (2)
O(5)-M-O(8)	70.5 (3)	71.2 (3)	71.1 (2)	71.6 (2)	70.2 (2)
O(6)-M-O(8)	71.6 (3)	72.5 (3)	71.9 (2)	72.2 (3)	72.3 (2)
O(7)-M-O(8)	141.2 (3)	141.7 (3)	141.6 (2)	141.2 (2)	141.9 (2)
O(1)-M-O(9)	73.4 (2)	72.3 (2)	72.7 (2)	72.8 (2)	72.6 (2)
O(2)-M-O(9)	87.0 (3)	86.8 (3)	86.7 (3)	86.7 (3)	86.3 (2)
O(3)-M-O(9)	67.7 (3)	67.0 (3)	66.7 (2)	66.9 (3)	66.4 (2)
O(4)-M-O(9)	77.5 (2)	77.6 (3)	78.0 (2)	78.1 (2)	78.0 (2)
O(5)-M-O(9)	143.0 (2)	142.1 (3)	142.2 (2)	141.9 (2)	142.5 (2)
O(6)-M-O(9)	129.0 (3)	129.7 (3)	130.5 (3)	130.6 (3)	130.8 (2)
O(7)-M-O(9)	71.9 (3)	73.4 (3)	73.2 (3)	73.4 (3)	73.2 (2)
O(8)-M-O(9)	139.6 (3)	138.5 (3)	138.8 (2)	138.6 (3)	138.9 (2)
M-O(1)-C(1)	119.4 (6)	120.0 (6)	119.8 (5)	120.4 (6)	120.3 (5)
M-O(2)-C(2)	116.8 (6)	117.0 (7)	116.0 (5)	117.2 (6)	116.0 (5)
M-O(2)-C(3)	122.9 (6)	121.7 (7)	123.7 (5)	122.3 (5)	123.4 (5)
C(2)-O(2)-C(3)	112.7 (8)	111.5 (9)	111.9 (7)	112.9 (7)	112.7 (7)
M-O(3)-C(4)	115.7 (6)	115.2 (6)	115.8 (5)	116.2 (5)	116.2 (5)
M-O(3)-C(5)	116.3 (6)	117.0 (6)	115.9 (5)	117.4 (5)	117.0 (5)
C(4)-O(3)-C(5)	113.9 (8)	112.0 (8)	112.4 (7)	111.3 (7)	111.9 (7)
M-O(4)-C(6)	119.4 (6)	120.1 (7)	119.6 (5)	120.7 (6)	121.5 (6)
O(1)-C(1)-C(2)	107.8 (9)	106.2 (9)	106.4 (7)	107.5 (7)	106.6 (7)
O(2)-C(2)-C(1)	110 (1)	110 (1)	109.6 (8)	108.9 (8)	109.4 (8)
O(2)-C(3)-C(4)	108.6 (9)	108.0 (9)	107.7 (7)	108.6 (8)	107.2 (8)
O(3)-C(4)-C(3)	109.4 (9)	105.9 (9)	107.5 (7)	106.2 (7)	106.9 (8)
O(3)-C(5)-C(6)	106.3 (9)	105.4 (9)	105.6 (8)	105.2 (8)	104.9 (8)
O(4)-C(6)-C(5)	109.7 (9)	108.8 (9)	108.8 (8)	108.2 (7)	107.7 (8)

clearly seen in Figure 2. One alcoholic EO3 oxygen atom (O(4)), one etheric oxygen atom (O(2)), and four water molecules (O(5,7-9)) form a trigonal prism with the water molecule, O(6), and EO3 oxygen atoms, O(1) and O(3), capping the three quadrilateral faces. The glycol oxygen atoms alternate along the acyclic chain from capping to prismatic sites. The O-C-C-O torsion angles are g^- (-60° , C(1)-C(2)), g^- (C(3)-C(4)), g^+ (C(5)-C(6)). The C-O-C-C angles are all "a" (180°) except for C(1)-C(2)-O(2)-C(3), which occurs between C-C torsion angles of like sign and deviates toward g^- (-108.6° for M = Nd). Representative

Table II. Torsion Angles (deg) for the Triethylene Glycol Ligands in Representative Complexes

atoms	M = Nd ^a	M = Dy ^b	M = Ho ^c	M = Er ^d	M = Lu ^e
O(1)-C(1)-C(2)-O(2)	-51.1	48.9	-49.9	49.6	51.7
C(1)-C(2)-O(2)-C(3)	-108.6	109.3	-166.6	153.4	169.2
C(2)-O(2)-C(3)-C(4)	-178.1	176.8	172.4	-174.1	-178.3
O(2)-C(3)-C(4)-O(3)	-49.9	51.0	54.8	-56.3	-52.8
C(3)-C(4)-O(3)-C(5)	-174.6	173.5	172.8	-177.0	
C(4)-O(3)-C(5)-C(6)	179.2	178.5	-173.3	173.1	
O(3)-C(5)-C(6)-O(4)	54.5	-52.1	-50.6	52.6	

^a $[M(OH_2)_5(EO_3)]Cl_3$. ^b $[M(OH_2)_5(EO_3)]Cl_3$ (opposite absolute configuration). ^c $[MCl_3(EO_3)] \cdot CH_3CN$. ^d $[MCl_3(EO_3)] \cdot OHMe$. ^e $[LuCl_3(EO_3)]$.

**Figure 3.** Hydrogen-bonding interactions to and from the formula unit in $[MCl_3(EO_3)] \cdot CH_3CN$ (M = Ho (shown), Lu).

values of the torsion angles for these complexes are given in Table II.

The glycol and water molecule hydrogen atoms interact with the chloride ions in a polymeric network of hydrogen bonding. There are 12 possible hydrogen atoms to participate in hydrogen bonds, and all 12 form single hydrogen bonds. Cl(1) accepts 5 hydrogen bonds, Cl(2) 4, and Cl(3) 3. The hydrogen bonding was inferred from O...Cl contact geometries. For M = Nd the O...Cl contacts range from 3.000 (6) to 3.287 (6) Å and the Cl...OH₂...Cl contact angles from 93.9 (2) to 116.6 (2)^o.

$[MCl_3(EO_3)] \cdot CH_3CN$ (M = Ho, Lu). The seven-coordinate distorted-pentagonal-bipyramidal geometry of these complexes is similar to that observed for $[MCl_3(EO_3)] \cdot 18$ -crown-6. There is no crystallographically imposed symmetry in these complexes, and the glycol ligand is ordered. The torsion angles around the acyclic ligand are as follows (starting with O(1)-C(1)-C(2)-O(2)): g^- (-60°), a (180°), a, g^+ , a, a, g^- . This sequence, with O-C-C-O angles alternating g^\pm and all C-O-C-C angles "a", is that found for the full-symmetry D_{3d} conformation of 18-crown-6.

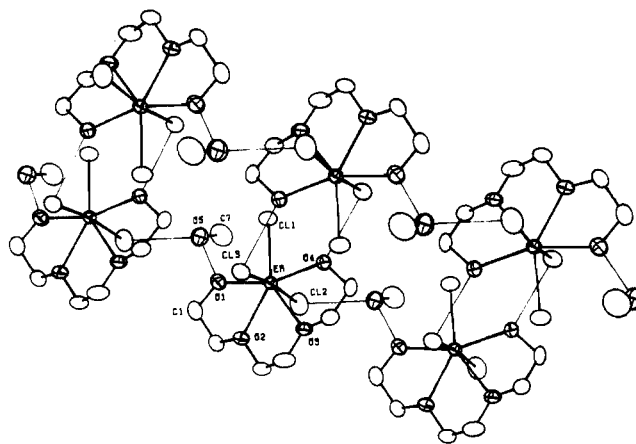
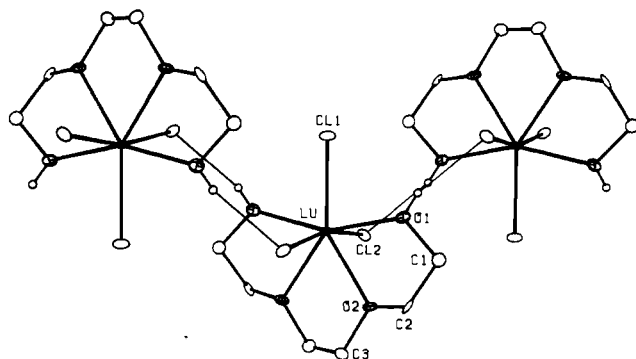
The glycol hydrogen atoms (located in a difference Fourier map) and acetonitrile hydrogen atoms participate in hydrogen bonds exclusively with the axial chlorine atoms Cl(2) and Cl(3). Cl(2) accepts one or possibly two hydrogen bonds from the solvent and one from O(1) (Figure 3, M = Ho). Cl(3) accepts one from C(8) and one from O(4). The interactions to and from Cl(3) and O(4) occur exclusively between two molecules related by $-x, 1 - y, 1 - z$. (O(4) of one donates to Cl(3) of the other and vice versa, forming a hydrogen-bonded dimer.) In the other interaction, O(1) donates to Cl(2) in a symmetry-related unit ($-x, y - 0.5, 0.5 - z$; M = Ho, H(1)[O(1)]...Cl(2) = 2.09 Å, O(1)...Cl(2) = 3.033 (4) Å) while Cl(2) in the same unit as O(1) accepts a hydrogen bond from O(1) related by $-x, 0.5 + y, 0.5 - z$ (M =

Table III. Bond Distances (Å) and Angles (deg) for $[\text{MCl}_3(\text{EO}_3)] \cdot \text{X}$ (M = Ho, Er, Yb, Lu; X = CH_3CN , OHMe)

	M = Ho, X = CH_3CN	M = Er, X = OHMe	M = Yb, X = OHMe	M = Lu, X = CH_3CN
M-Cl(1)	2.571 (1)	2.565 (2)	2.546 (3)	2.537 (2)
M-Cl(2)	2.616 (1)	2.589 (2)	2.572 (4)	2.573 (2)
M-Cl(3)	2.615 (1)	2.615 (2)	2.597 (3)	2.563 (2)
M-O(1)	2.331 (4)	2.318 (5)	2.301 (7)	2.270 (6)
M-O(2)	2.393 (4)	2.380 (5)	2.356 (7)	2.348 (6)
M-O(3)	2.404 (4)	2.414 (5)	2.395 (7)	2.352 (6)
M-O(4)	2.330 (4)	2.328 (5)	2.323 (6)	2.286 (5)
O(1)-C(1)	1.449 (7)	1.42 (1)	1.42 (1)	1.47 (1)
O(2)-C(2)	1.436 (7)	1.465 (9)	1.46 (1)	1.45 (1)
O(2)-C(3)	1.443 (7)	1.43 (1)	1.45 (1)	1.46 (1)
O(3)-C(4)	1.443 (7)	1.43 (1)	1.38 (1)	1.43 (1)
O(3)-C(5)	1.433 (7)	1.436 (9)	1.47 (1)	1.45 (1)
O(4)-C(6)	1.446 (7)	1.46 (1)	1.47 (1)	1.45 (1)
C(1)-C(2)	1.508 (8)	1.50 (1)	1.52 (2)	1.52 (1)
C(3)-C(4)	1.484 (9)	1.49 (1)	1.53 (2)	1.48 (1)
C(5)-C(6)	1.500 (8)	1.52 (1)	1.52 (2)	1.51 (1)
N-C(7)	1.19 (1)			1.18 (2)
C(7)-C(8)	1.42 (1)			1.44 (2)
O(5)-C(7)		1.50 (2)	1.47 (2)	
O(5')-C(7)		1.33 (2)	1.30 (3)	
Cl(1)-M-Cl(2)	94.56 (5)	96.38 (8)	96.2 (1)	94.78 (8)
Cl(1)-M-Cl(3)	95.98 (5)	93.78 (7)	94.1 (1)	95.48 (8)
Cl(2)-M-Cl(3)	169.43 (5)	169.82 (7)	169.7 (1)	169.73 (8)
Cl(1)-M-O(1)	80.8 (1)	80.2 (1)	79.7 (2)	79.5 (2)
Cl(2)-M-O(1)	91.1 (1)	90.3 (2)	89.9 (2)	91.2 (2)
Cl(3)-M-O(1)	91.5 (1)	92.1 (2)	92.5 (2)	91.3 (2)
Cl(1)-M-O(2)	146.7 (1)	146.9 (1)	146.5 (2)	146.4 (2)
Cl(2)-M-O(2)	85.3 (1)	87.3 (1)	87.2 (2)	84.8 (2)
Cl(3)-M-O(2)	86.4 (1)	84.5 (1)	84.6 (2)	86.9 (2)
O(1)-M-O(2)	65.9 (1)	66.9 (2)	66.9 (2)	66.9 (2)
Cl(1)-M-O(3)	147.6 (1)	146.5 (1)	147.0 (2)	147.4 (1)
Cl(2)-M-O(3)	85.23 (9)	86.6 (1)	87.1 (2)	85.3 (2)
Cl(3)-M-O(3)	85.40 (9)	84.6 (1)	84.0 (2)	85.7 (2)
O(1)-M-O(3)	131.6 (1)	133.3 (2)	133.2 (3)	133.1 (2)
O(2)-M-O(3)	65.7 (1)	66.5 (2)	66.3 (2)	66.2 (2)
Cl(1)-M-O(4)	81.0 (1)	79.5 (1)	79.2 (2)	79.9 (2)
Cl(2)-M-O(4)	90.4 (1)	92.6 (1)	92.8 (2)	90.8 (2)
Cl(3)-M-O(4)	90.3 (1)	88.7 (1)	88.5 (2)	90.4 (2)
O(1)-M-O(4)	161.8 (1)	159.7 (2)	158.9 (3)	159.4 (2)
O(2)-M-O(4)	132.3 (1)	133.4 (2)	134.1 (2)	133.7 (2)
O(3)-M-O(4)	66.6 (1)	67.0 (2)	67.9 (2)	67.5 (2)
M-O(1)-C(1)	122.8 (4)	121.3 (5)	121.2 (6)	121.5 (5)
M-O(2)-C(2)	116.9 (4)	116.3 (4)	117.6 (6)	116.4 (5)
M-O(2)-C(3)	118.9 (3)	117.8 (4)	117.3 (6)	119.0 (5)
C(2)-O(2)-C(3)	114.6 (5)	113.5 (6)	111.6 (8)	112.7 (7)
M-O(3)-C(4)	117.2 (3)	116.3 (5)	117.6 (7)	118.4 (5)
M-O(3)-C(5)	116.3 (3)	115.8 (4)	115.0 (6)	116.8 (5)
C(4)-O(3)-C(5)	113.0 (5)	113.0 (6)	113.1 (9)	112.2 (7)
M-O(4)-C(6)	121.0 (3)	120.4 (4)	120.7 (6)	121.4 (5)
O(1)-C(1)-C(2)	104.6 (5)	108.2 (7)	108.3 (9)	103.6 (8)
O(2)-C(2)-C(1)	106.8 (5)	104.7 (7)	102.4 (9)	102.4 (8)
O(2)-C(3)-C(4)	105.9 (5)	106.1 (7)	104 (1)	104.7 (8)
O(3)-C(4)-C(3)	105.6 (5)	105.9 (6)	105 (1)	105.4 (8)
O(3)-C(5)-C(6)	106.2 (5)	104.8 (6)	106.0 (9)	105.3 (7)
O(4)-C(6)-C(5)	106.8 (5)	106.8 (6)	106.0 (8)	105.9 (7)
N-C(7)-C(8)	176 (1)			178 (2)

Ho, $\text{H}(1)[\text{O}(4)] \cdots \text{Cl}(3) = 2.08 \text{ \AA}$, $\text{O}(4) \cdots \text{Cl}(3) = 3.085 (5) \text{ \AA}$. This interaction thus creates polymeric chains of hydrogen-bonded dimers propagating along *b*. These chains are interconnected by the solvent interactions (M = Ho, $\text{C}(8) \cdots \text{Cl}(2) = 3.645 (9) \text{ \AA}$, $\text{C}(8) \cdots \text{Cl}(3) = 3.80 (1) \text{ \AA}$). Bond distances and angles for the two complexes of this type that have been structurally characterized are given in Table III.

$[\text{MCl}_3(\text{EO}_3)] \cdot \text{OHMe}$ (M = Er, Yb). The distorted-pentagonal-bipyramidal geometry of the metal ion in these two complexes is essentially identical with that found for the complexes above and the 18-crown-6 adducts. The inclusion of a solvent molecule that can accept as well as donate hydrogen bonds results in a more symmetric overall structure as depicted in Figure 4 (M = Er). The solvent oxygen (O(5)) bridges formula units related by a unit

**Figure 4.** Portions of the hydrogen-bonded polymeric chains in $[\text{MCl}_3(\text{EO}_3)] \cdot \text{OHMe}$ (M = Er (shown), Yb) which propagate along *a*.**Figure 5.** Portion of the hydrogen-bonded zigzag polymeric chain in $[\text{LuCl}_3(\text{EO}_3)]$ propagating along *c*.

translation along *a*, by accepting a hydrogen bond from glycol oxygen O(1) (M = Er, $\text{O}(1) \cdots \text{O}(5), \text{O}(5)' = 2.58 (1), 2.53 (2) \text{ \AA}$) and donating a hydrogen bond to Cl(2) in a symmetry-related unit (M = Er, $\text{O}(5), \text{O}(5)' \cdots \text{Cl}(2) = 3.02 (2), 3.20 (2) \text{ \AA}$). The chains along *a* are bridged by complementary hydrogen bonds between O(4) and Cl(3) (M = Er, $\text{O}(4) \cdots \text{Cl}(3) = 3.078 (5) \text{ \AA}$). Thus there are two hydrogen bonds between formula units related by the centers of symmetry (O(4) of one to Cl(3) of the other ($-x, 1-y, -z$) and vice versa). Cl(3) has only one hydrogen-bonding interaction, while Cl(1) has none. The overall structure can thus be described as pairs of parallel hydrogen-bonded chains propagating along *a*.

Bond distances and angles for these two complexes are included in Table III. The metal to axial chlorine bond distances show distinct differences related to the different hydrogen-bonding environments of Cl(2) versus Cl(3). The glycol ligand again adopts the symmetric conformation where O-C-C-O torsion angles alternate g^\pm and the C-O-C-C angles are all "a" (Table II). The solvent molecule is disordered.

$[\text{LuCl}_3(\text{EO}_3)]$. This anhydrous, unsolvated complex is depicted in Figure 5. This is the most symmetric of the hydrogen-bonded structures in this series. The Lu atom resides on a 2-fold axis with the equatorial chlorine, Cl(1). The seven-coordinate distorted pentagonal bipyramids form hydrogen-bonded zigzag chains along the unit cell axis *c* (all hydrogen atoms were located, $\text{H}(1)[\text{O}(1)] \cdots \text{Cl}(2) = 2.35 \text{ \AA}$, $\text{O}(1)-\text{H}(1)[\text{O}(1)] \cdots \text{Cl}(2) = 153^\circ$, $\text{O}(1) \cdots \text{Cl}(2) = 3.084 (5) \text{ \AA}$). The formula units hydrogen bonded to each other are related by centers of symmetry. Unlike the case for the solvates and 18-crown-6 adducts, both interactions to the axial chlorines are donated by the same formula units accepting the glycol oxygen-hydrogen bonds. Thus, each axial chlorine has only one hydrogen-bonding interaction and each pentagonal-bipyramidal unit interacts with only two others (the two other metal centers are related by a unit translation along *c*).

The bond distances and angles for this complex are presented in Table IV. The O-C-C-O torsion angles alternate g^\pm , and the

Table IV. Bond Distances (Å) and Angles (deg) for [LuCl₃(EO3)]

Lu-Cl(1)	2.547 (2)	Lu-Cl(2)	2.584 (2)
Lu-O(1)	2.279 (5)	Lu-O(2)	2.351 (5)
O(1)-C(1)	1.470 (8)	O(2)-C(2)	1.451 (8)
O(2)-C(3)	1.470 (9)	C(1)-C(2)	1.48 (1)
C(3)-C(3)	1.48 (2)		
Cl(1)-Lu-Cl(2)	96.93 (4)	Cl(1)-Lu-O(1)	78.3 (1)
Cl(2)-Lu-O(1)	91.6 (1)	Cl(1)-Lu-O(2)	146.1 (1)
Cl(2)-Lu-O(2)	84.0 (1)	O(1)-Lu-O(2)	67.7 (2)
Cl(2)-Lu-Cl(2) ^a	166.14 (8)	Cl(2)-Lu-O(1) ^a	91.2 (1)
Cl(2)-Lu-O(2) ^a	84.5 (1)	O(1)-Lu-O(1) ^a	156.7 (3)
O(1)-Lu-O(2) ^a	135.6 (2)	O(2)-Lu-O(2) ^a	67.9 (3)
Lu-O(1)-C(1)	120.8 (4)	Lu-O(2)-C(2)	114.7 (4)
Lu-O(2)-C(3)	117.5 (4)	C(2)-O(2)-C(3)	114.1 (5)
O(1)-C(1)-C(2)	105.9 (6)	O(2)-C(2)-C(1)	105.5 (6)
O(2)-C(3)-C(3) ^a	106.3 (5)		

^a Atoms related by the crystallographic 2-fold axis.

C-O-C-C torsion angles are all "a" (Table II).

Discussion

Anhydrous, unsolvated 1:1 complexes of the lanthanide chlorides (La-Lu, Y) and triethylene glycol were prepared by Hirashima by first dehydrating the solution of hydrated salt and ligand and then drying the precipitate in vacuo at elevated temperatures.¹⁹ We, on the other hand, have been interested in the effects of small amounts of water on complexation and the resulting structure, and thus we have attempted these reactions without any special drying or harsh conditions. This approach should yield valuable clues to the nature of complexation in these systems, especially if they are ever to be considered as separations agents from environmental (aqueous) solutions.

As it turns out, small amounts of water have pronounced effects on the structures of the early- to mid-lanthanide systems, which crystallize as the pentahydrates, [M(OH₂)₅(EO3)]Cl₃ (M = Nd, Eu, Gd, Dy, Y have been structurally characterized; M = Sm has been isolated). Yields of these complexes have been highest for the early lanthanides and tend to decrease as the metal ion size decreases. This trend has also been observed by Hirashima for polyethylene glycol complexes of lanthanide nitrates^{13,14,18} and chlorides.¹⁹ In our systems, M = Eu and Gd crystallize in generous

quantities overnight. The Dy and Y systems take several days, and then yields are very low.

An interesting difference in the reactions with early lanthanides La, Ce, Nd, and Sm has been observed versus the reactions with mid-series lanthanides Eu-Dy and Y. After they are heated at 60 °C for 1 h and cooled to room temperature, the early lanthanides all form a two-layer clathrate system, with the bottom layer being a very viscous solution. When a vacuum is placed on these systems and the volume reduced, precipitation occurs almost immediately. Suitable crystals for the X-ray diffraction studies were obtained in this fashion for M = Nd; however, M = La came out as a powder and M = Sm as twinned crystals. Crystals of the pentahydrates are deliquescent but dissolve much more slowly (1 to 5h with high humidity) than the complexes of the later lanthanides.

We suspect that water interferes with the crystallization of the later lanthanide systems as observed by Hirashima.^{13,14,18,19} First, yields of the seven-coordinate complexes [MCl₃(EO3)]·X (M = Ho, Er, Yb, Lu; X = CH₃CN, OHMe) have been very low except when we prepared the ytterbium complex from the anhydrous salt. In this reaction copious quantities of huge transparent blocks (1.5 mm on edge) formed overnight. Second, our experience with complexation reactions of later lanthanide chlorides and crown ethers has shown us a definite trend toward formation of octa-aquated metal ions hydrogen-bonded to chloride ions and the crown ether. Examples of this include [Dy(OH₂)₈]Cl₃·18-crown-6·4H₂O,¹ [Lu(OH₂)₈]Cl₃·1.5(12-crown-4)·2H₂O,² and [M(OH₂)₈]Cl₃·15-crown-5 (M = Y,^{5,7} Gd,⁶ Lu⁶). It may not be unreasonable to assume that the octa-aquated ion forms to some degree in our systems of late lanthanides but that the hydrogen bond donating ability in addition to hydrogen bond acceptance in the triethylene glycol ligand prevents the formation of well-ordered crystalline complexes as observed for the crown ethers. The late-lanthanide ions, then, may accept complexation to triethylene glycol as an acceptable "second choice". In any case the anhydrous complexes formed are extremely deliquescent and dissolve within 1 min when exposed to the humidity in air.

We must mention at this point the use of LiCl to prepare anhydrous derivatives of the early- to mid-series lanthanides. While attempting to isolate new, anhydrous 18-crown-6 complexes of Dy and YCl₃, we "accidentally" crystallized [MCl₃(EO3)]·

Table V. Comparison of Bonding Parameters in Lanthanide Triethylene Glycol Complexes

complex	CN	IR ^a	G ^b	M-EO ₃ (av), ^c Å								ref		
				M-Cl(av), Å		M-OH ₂ (av), Å		capping		others				
				ax	eq	capping	others	a	e	a	e			
[M(OH ₂) ₅ (EO3)]Cl ₃														
M = Nd	9	1.163	tctp			2.506 (7)	2.500 (8)	2.480 (7)	2.596 (7)	2.469 (7)	2.500 (8)			this study
M = Eu ^d	9	1.120	tctp			2.483 (8)	2.452 (3)	2.457 (7)	2.577 (7)	2.426 (7)	2.471 (9)			
M = Gd	9	1.107	tctp			2.455 (6)	2.451 (7)	2.440 (5)	2.564 (6)	2.408 (5)	2.466 (7)			
M = Dy	9	1.083	tctp			2.428 (6)	2.41 (1)	2.416 (6)	2.539 (6)	2.373 (6)	2.445 (7)			
M = Y	9	1.075	tctp			2.437 (6)	2.409 (7)	2.420 (5)	2.544 (6)	2.376 (6)	2.439 (6)			
[MCl ₃ (EO3)]·18-crown-6														
M = Dy ^d	7	0.97	pbp	2.626 (2)	2.605 (2)					2.331 (4)	2.442 (5)			this study
M = Y	7	0.96	pbp	2.611 (2)	2.588 (3)					2.326 (5)	2.431 (5)			
M = Y ^d	7	0.96	pbp	2.622 (2)	2.595 (3)					2.306 (5)	2.435 (5)			
[MCl ₃ (EO3)]·CH ₃ CN														
M = Ho	7	0.96 ^e	pbp	2.616 (1)	2.571 (1)					2.330 (1)	2.398 (6)			this study
M = Lu	7	0.92 ^e	pbp	2.568 (5)	2.537 (2)					2.278 (8)	2.350 (2)			
[MCl ₃ (EO3)]·OHMe														
M = Er	7	0.945	pbp	2.60 (1)	2.565 (2)					2.323 (5)	2.40 (2)			this study
M = Yb	7	0.925	pbp	2.58 (1)	2.546 (3)					2.31 (1)	2.38 (2)			
[LuCl ₃ (EO3)] ^d	7	0.92 ^e	pbp	2.584 (2)	2.547 (2)					2.279 (5)	2.351 (5)			this study
[M(NO ₃) ₃ (EO3)]														
M = Nd	10	1.22 ^e								2.50 (1)	2.52 (2)			17
M = Eu	10	1.17 ^e								2.45 (2)	2.502 (7)			20
[M(NO ₃) ₃ (EO ₄)]														
M = La	11	1.32 ^e								2.58 (3)	2.70 (3)			21
M = Nd	10	1.22 ^e								2.51 (3)	2.65 (4)			15
[Nd(NO ₃) ₂ (EO5)][NO ₃]	10	1.22 ^e								2.485 (3)	2.59 (3)			16

^a Ionic radius for M³⁺ and CN shown from ref 25. ^b Coordination geometries: tctp = tricapped trigonal prism, pbp = pentagonal bipyramid. ^c Symbols a and e refer to alcoholic and etheric oxygen atoms, respectively. ^d Crystal structure determination at -150 °C. ^e Extrapolated from data in ref 25.

Table VI. Crystal Data and Summary of Intensity Data Collection and Structure Refinement

	[MCl ₃ (EO ₃)]-18-crown-6			
	M = Y (20 °C)	M = Y (-150 °C)	M = Dy	[M(OH ₂) ₅ (EO ₃)]Cl ₃ M = Nd
color/shape	colorless/parallelepiped	colorless/parallelepiped	colorless/parallelepiped	pink/fragment
mol wt	609.8	609.8	683.4	490.8
space group	<i>C2/c</i>	<i>C2/c</i>	<i>C2/c</i>	<i>Pna2</i> ₁
temp, °C	20	-150	-150	20
cell constants ^a	$\theta > 20^\circ$	$\theta > 20^\circ$ (15 rflns)	$\theta > 20^\circ$	$\theta > 24^\circ$
<i>a</i> , Å	16.606 (5)	16.352 (4)	16.361 (5)	14.463 (2)
<i>b</i> , Å	13.786 (4)	13.600 (5)	13.620 (1)	9.746 (1)
<i>c</i> , Å	11.830 (5)	11.890 (3)	11.889 (3)	12.224 (1)
β , deg	92.42 (3)	92.54 (2)	92.28 (2)	
cell vol, Å ³	2706.1	2641.4	2647.2	1723
formula units/unit cell	4	4	4	4
<i>D</i> _{calcd} , g cm ⁻³	1.50	1.53	1.71	1.89
μ (calcd), cm ⁻¹	24.8	24.8	30.1	41.3
diffractometer/scan	Enraf-Nonius CAD4/ θ -2 θ	Enraf-Nonius CAD4/ θ -2 θ	Enraf-Nonius CAD4/ θ -2 θ	Enraf-Nonius CAD4/ θ -2 θ
range of rel transmission factors, %	71-100	76-100	90-100	78-100
radiation (graphite monochromatized)	Mo K α ($\lambda = 0.71073$ Å)	Mo K α ($\lambda = 0.71073$ Å)	Mo K α ($\lambda = 0.71073$ Å)	Mo K α ($\lambda = 0.71073$ Å)
max cryst dimens, mm	0.21 × 0.41 × 0.55	0.21 × 0.41 × 0.55	0.08 × 0.13 × 0.23	0.28 × 0.33 × 0.45
scan width	0.80 + 0.35 tan θ	0.80 + 0.35 tan θ	0.80 + 0.35 tan θ	0.80 + 0.35 tan θ
std rflns	(12,0,0), (0,10,0), (008)	(12,0,0), (0,10,0), (008)	(10,0,0), (080), (006)	(14,0,0), (080), (0,0,14)
decay of stds, %	±3	±2	±3	±2
rflns measd	2567	2545	2547	1773
2 θ range, deg	2 ≤ 2 θ ≤ 50	2 ≤ 2 θ ≤ 50	2 ≤ 2 θ ≤ 50	2 ≤ 2 θ ≤ 50
range of <i>hkl</i>	+19,+16,±14	±19,+16,+14	±19,+16,+14	+17,+11,+14
rflns obsd [<i>F</i> _o ≥ 5 σ (<i>F</i> _o)] ^b	1571	1915	2027	1559
computer programs	SHELX ²⁶	SHELX ²⁶	SHELX ²⁶	SHELX ²⁶
structure soln	coordinates from M = Dy	coordinates from M = Y (20 °C)	heavy-atom techniques	coordinates from M = Gd
no. of params varied	143	143	143	171
wts	[σ (<i>F</i> _o) ²] ⁻¹	[σ (<i>F</i> _o) ²] ⁻¹	[σ (<i>F</i> _o) ²] ⁻¹	[σ (<i>F</i> _o) ²] ⁻¹
GOF	1.93	3.80	1.28	4.00
<i>R</i> = $\sum F_o - F_c / \sum F_o $	0.052	0.053	0.036	0.026
<i>R</i> _w	0.055	0.060	0.038	0.027
<i>R</i> of inverse config				0.030
largest feature in final diff map, e Å ⁻¹	0.5	0.9	1.0	0.8

	[M(OH ₂) ₅ (EO ₃)]Cl ₃			
	M = Eu	M = Gd	M = Dy	M = Y
color/shape	colorless/plate	colorless/parallelepiped	colorless/cube	colorless/fragment
mol wt	498.6	503.9	509.1	435.5
space group	<i>Pna2</i> ₁	<i>Pna2</i> ₁	<i>Pna2</i> ₁	<i>Pna2</i> ₁
temp, °C	-150	20	20	20
cell constants ^a	$\theta > 19^\circ$	$\theta > 22^\circ$	$\theta > 22^\circ$	$\theta > 21^\circ$ (21 rflns)
<i>a</i> , Å	14.330 (2)	14.344 (1)	14.282 (2)	14.256 (2)
<i>b</i> , Å	9.679 (1)	9.708 (1)	9.687 (1)	9.675 (1)
<i>c</i> , Å	12.107 (1)	12.154 (2)	12.121 (1)	12.104 (1)
cell vol, Å ³	1679	1692	1677	1669
formula units/unit cell	4	4	4	4
<i>D</i> _{calcd} , g cm ⁻³	1.97	1.98	2.02	1.73
μ (calcd), cm ⁻¹	40.1	42.0	47.2	39.1
diffractometer/scan	Enraf-Nonius CAD4/ θ -2 θ	Enraf-Nonius CAD4/ θ -2 θ	Enraf-Nonius CAD4/ θ -2 θ	Enraf-Nonius CAD4/ θ -2 θ
range of rel transmission factors, %	67-100	92-100	80-100	67-100
radiation (graphite monochromatized)	Mo K α ($\lambda = 0.71073$ Å)	Mo K α ($\lambda = 0.71073$ Å)	Mo K α ($\lambda = 0.71073$ Å)	Mo K α ($\lambda = 0.71073$ Å)
max cryst dimens, mm	0.10 × 0.20 × 0.20	0.20 × 0.23 × 0.35	0.18 × 0.25 × 0.25	0.20 × 0.30 × 0.38
scan width	0.80 + 0.35 tan θ	0.80 + 0.35 tan θ	0.80 + 0.35 tan θ	0.80 + 0.35 tan θ
std rflns	(10,0,0), (080), (0,0,10)	(12,0,0), (040), (0,0,12)	(12,0,0), (080), (0,0,12)	(10,0,0), (080), (0,0,10)
decay of stds, %	±0.9	±2	±2	±3
rflns measd	1717	1733	1716	1708
2 θ range, deg	2 ≤ 2 θ ≤ 50	2 ≤ 2 θ ≤ 50	2 ≤ 2 θ ≤ 50	2 ≤ 2 θ ≤ 50
range of <i>hkl</i>	+17,+11,+14	+17,+11,+14	+17,+11,+14	+16,+11,+14
rflns obsd [<i>F</i> _o ≥ 5 σ (<i>F</i> _o)] ^b	1395	1502	1470	1319
computer programs ^c	SHELX ²⁶	SHELX ²⁶	SHELX ²⁶	SHELX ²⁶
structure soln	coordinates from M = Gd	heavy-atom techniques	coordinates from M = Gd	coordinates from M = Gd
no. of params varied	166	171	171	171
wts	[σ (<i>F</i> _o) ²] ⁻¹	[σ (<i>F</i> _o) ²] ⁻¹	[σ (<i>F</i> _o) ²] ⁻¹	[σ (<i>F</i> _o) ² + 0.00002 <i>F</i> _o ²] ⁻¹
GOF	2.57	3.42	2.82	2.42
<i>R</i> = $\sum F_o - F_c / \sum F_o $	0.031	0.023	0.023	0.034
<i>R</i> _w	0.032	0.026	0.025	0.035
<i>R</i> of inverse config	0.038	0.028	0.028	0.053
largest feature in final diff map, e Å ⁻¹	1.0	0.6	0.6	0.5

Table VI (Continued)

	[MCl ₃ (EO ₃)]·CH ₃ CN		[MCl ₃ (EO ₃)]·OHMe		[LuCl ₃ (EO ₃)]
	M = Ho	M = Lu	M = Er	M = Yb	
color/shape	peach/ parallelepiped	colorless/ fragment	pink/ parallelepiped	colorless/ fragment	colorless/ parallelepiped
mol wt	462.5	472.6	455.8	461.6	431.5
space group	<i>P</i> 2 ₁ / <i>c</i>	<i>P</i> 2 ₁ / <i>c</i>	<i>P</i> 2 ₁ / <i>c</i>	<i>P</i> 2 ₁ / <i>c</i>	<i>Pbcn</i>
temp, °C	20	20	20	20	-150
cell constants ^a	$\theta > 23^\circ$	$\theta > 21^\circ$	$\theta > 23^\circ$	$\theta > 24^\circ$	$\theta > 24^\circ$
<i>a</i> , Å	9.048 (2)	8.999 (2)	7.460 (2)	7.440 (1)	7.5893 (6)
<i>b</i> , Å	10.904 (1)	10.792 (5)	14.402 (5)	14.350 (4)	11.130 (1)
<i>c</i> , Å	16.434 (2)	16.338 (3)	14.220 (2)	14.214 (4)	14.802 (2)
β , deg	103.96 (2)	103.80 (2)	101.93 (2)	102.10 (2)	
cell vol, Å ³	1574	1541	1495	1484	1250.3
formula units/unit cell	4	4	4	4	4
<i>D</i> _{calcd} , g cm ⁻³	1.95	2.04	2.02	2.07	2.29
μ (calcd), cm ⁻¹	52.8	66.2	58.6	65.4	81.5
diffractometer/scan	Enraf-Nonius CAD4/ θ -2 θ	Enraf-Nonius CAD4/ θ -2 θ	Enraf-Nonius CAD4/ θ -2 θ	Enraf-Nonius CAD4/ θ -2 θ	Enraf-Nonius CAD4/ θ -2 θ
range of rel transmission factors, %	49.8-100	49-100	49-100	29-100	83-100
radiation (graphite monochromatized)	Mo K α (λ = 0.71073 Å)	Mo K α (λ = 0.71073 Å)	Mo K α (λ = 0.71073 Å)	Mo K α (λ = 0.71073 Å)	Mo K α (λ = 0.71073 Å)
max cryst dimens, mm	0.30 × 0.40 × 0.50	0.40 × 0.65 × 0.95	0.25 × 0.35 × 0.53	0.22 × 0.52 × 0.60	0.20 × 0.35 × 0.25
scan width	0.80 + 0.35 tan θ	0.80 + 0.35 tan θ	0.80 + 0.35 tan θ	0.80 + 0.35 tan θ	0.80 + 0.35 tan θ
std rflns	(900), (0,10,0), (0,0,14)	(900), (0,10,0), (0,0,14)	(700), (0,14,0), (0,0,10)	(700), (0,16,0), (0,0,10)	(800), (0,12,0), (0,0,14)
decay of stds, %	-4	-3.4	±1.4	±1	±1.4
rflns measd	3101	3039	2946	2925	1300
2 θ range, deg	2 ≤ 2 θ ≤ 50	2 ≤ 2 θ ≤ 50	2 ≤ 2 θ ≤ 50	2 ≤ 2 θ ≤ 50	2 ≤ 2 θ ≤ 50
range of <i>hkl</i>	+10,+12,±19	+10,+12,±19	+8,+17,±16	+8,+17,±16	+9,+13,+17
rflns obsd [<i>F</i> _o ≥ 5 σ (<i>F</i> _o)] ^b	2486	2505	2299	2310	859
computer programs ^c	SHELX ²⁶	SHELX ²⁶	SHELX ²⁶	SHELX ²⁶	SHELX ²⁶
structure soln	heavy-atom techniques	coordinates from M = Ho	heavy-atom techniques	coordinates from M = Er	heavy-atom techniques
no. of params varied	154	154	154	154	60
wts	[σ (<i>F</i> _o) ²] ⁻¹	[σ (<i>F</i> _o) ²] ⁻¹	[σ (<i>F</i> _o) ²] ⁻¹	[σ (<i>F</i> _o) ²] ⁻¹	[σ (<i>F</i> _o) ²] ⁻¹
GOF	1.40	6.60	2.80	4.25	2.10
<i>R</i> = $\sum F_o - F_c / \sum F_o $	0.028	0.035	0.032	0.042	0.030
<i>R</i> _w	0.028	0.041	0.036	0.049	0.032
<i>R</i> of inverse config					
largest feature in final diff map, e Å ⁻¹	0.6	0.8, 1.6 Å from Lu	0.7 H(1)[O(4)]	1.0 H(1)[O(4)]	0.9

^aLeast-squares refinement of $((\sin \theta)/\lambda)^2$ values for 25 reflections with θ greater than shown. ^bCorrections: Lorentz polarization, and absorption (empirical, ψ scan). ^cNeutral atom scattering factors and anomalous dispersion corrections from ref 27.

18-crown-6. (Our use of LiCl is briefly mentioned in ref 9.) We feel that this may be an easy route to complexes of the early- to mid-series lanthanides similar to complexes observed past M = Ho. These reactions are currently under investigation.

Only two major types of complexes have been crystallized and structurally characterized, the nine-coordinate pentahydrates [M(OH₂)₅(EO₃)Cl₃] (M = Nd, Eu, Gd, Dy, Y) and the seven-coordinate solvated [MCl₃(EO₃)]·X (M = Ho, Lu, X = CH₃CN; M = Er, Yb, X = OHMe) or unsolvated [LuCl₃(EO₃)] complexes. A comparison of the coordination parameters for all structurally characterized complexes is presented in Table V; representative torsion angles for the triethylene glycol ligands are presented in Table II.

It is not unreasonable to assume that a coordination number of 7 is too low for the early lanthanides and that these ions prefer the observed coordination number of 9. The presence of five water molecules in these complexes probably prevents any tight ion pairs between the metal and chloride ions. The water molecules stabilize the cations by coordination and the chloride ions by hydrogen bonding. The fact that the EO₃ ligand occupies four coordination sites yet donates only two hydrogen bonds may be a major factor dictating the preference of the lanthanide ions for water molecules. Without the hydrogen bonding from water molecules the late-lanthanide complexes all crystallize with three tight ion pairs.

The triethylene glycol ligand adopts a different conformation in the nine-coordinate versus that in the seven-coordinate complexes. In the nine-coordinate species the glycol oxygen atoms alternate from prismatic to capping coordination sites with one

alcoholic and one etheric oxygen of each type. This necessitates a deformation in one of the C-O-C-C torsion angles away from anti (180°) and toward gauche (±60°). All four oxygen atoms are in equivalent equatorial coordination sites in the seven-coordinate complexes, and the torsion angles reveal an identical, highly symmetrical conformation for all of these complexes. The O-C-C-O angles alternate *g*[±] and the C-O-C-C angles are all "a" as observed in the full-symmetry *D*_{3d} conformation of 18-crown-6.

Trends in the bond distances given in Table V are not unexpected: the distances decrease with increasing atomic number of the metal, and the seven-coordinate complexes exhibit shorter M-O separations than the nine-coordinate moieties. For a given coordination site the alcoholic oxygen to metal distance is shorter than the etheric oxygen to metal separation and the capping distances are longer than the prismatic sites in the nine-coordinate complexes. It is interesting to note that for a given coordination site the M-O(alcoholic) distances tend to be shorter than the M-OH₂ separations and the M-O(etheric) distances longer (although for M = Nd the last two values are equal). These parameters can be compared with the nine-coordinate M-O(18-crown-6) lengths in [GdCl(OH₂)₅(18-crown-6)]Cl₂·2H₂O (2.52 (3) Å)⁸ and [M(OH₂)₇(OHMe)][MCl(OH₂)₂(18-crown-6)]₂Cl₇·2H₂O (M = Y, 2.44 (5) Å; M = Dy, 2.46 (5) Å).⁹ In the crown ether structures the less flexible crown ether molecule exhibits greater deformations in the nine-coordinate tricapped-trigonal-prismatic coordination geometry than observed for the flexible EO₃ ligand. Coordination distances for other polyethylene

glycol complexes of lanthanide ions are given in Table V.

A final point of crystallographic interest involves the hydrogen-bonding patterns in the seven-coordinate triethylene glycol complexes. In $[\text{MCl}_3(\text{EO}_3)]\cdot 18\text{-crown-6}$, the presence of oxygen atoms in the crown ether to accept the glycol hydrogen bonds precludes any interaction with the chlorine atoms and linear polymeric chains result. Acetonitrile weakly interacts with both axial chlorines to bridge chains in the $[\text{MCl}_3(\text{EO}_3)]\cdot \text{CH}_3\text{CN}$ structures already connected via glycol hydrogen bonds to each of the axial ligands. The solvent is readily lost to yield an amorphous powder of the unsolvated complex. The solvent interactions are much stronger in the methanol solvates, where the methanol accepts a glycol hydrogen bond and donates one to one of the axial chlorines while the other axial ligand accepts a glycol hydrogen bond. These structures are the only ones where the axial chlorine atoms have substantially different environments, and this is reflected in the M–Cl separations. With $[\text{ErCl}_3(\text{EO}_3)]\cdot \text{OHMe}$ as an example, the Er–Cl(2) distance (2.589 (2) Å, solvent hydrogen bond acceptor) is significantly shorter than the Er–Cl(3) separation (2.615 (2) Å, glycol hydrogen bond acceptor). In all of the other structures the M–Cl(axial) distances are nearly equivalent.

The anhydrous, solvent-free $[\text{LuCl}_3(\text{EO}_3)]$ exhibits hydrogen bonds exclusively from glycol oxygen atoms to axial chlorines. For both axial and equatorial sites the Lu–Cl separations in this complex are longer than observed in $[\text{LuCl}_3(\text{EO}_3)]\cdot \text{CH}_3\text{CN}$ (the former was characterized at -150°C).

Conclusions

If we assume that a chloride ion can easily support four hydrogen bonds in a tetrahedral array, 3 chloride ions would require 12 hydrogen bonds. Triethylene glycol can supply 2, and 5 water molecules would be required for the other 10 in this ideal situation. It is not surprising then that the pentahydrates form for the early- and mid-series lanthanides, which can easily support a coordination number of 9. As the size of the lanthanide decreases, it becomes harder to support high coordination numbers, and in the complexes reported here, a structural change to seven-coordination occurs at $\text{M} = \text{Ho}$. It may be possible to modify the nine-coordinate complexes via interaction with the Cl^- counterion, and we are pursuing that line of investigation.

The differences observed in hydrogen bonding in the solvates may be responsible for the observed differences in crystallization. The acetonitrile adducts formed when precipitates were washed with cold acetonitrile only. The methanol solvates crystallized from 3:1 solutions of acetonitrile and methanol and exhibit much stronger interactions.

Triethylene glycol may prove to be an easy route to anhydrous soluble lanthanide chlorides for the later lanthanide ions. We intend to use this route to make novel organometallic complexes of the late-lanthanide metals.

Experimental Section

Synthesis and Crystallization of $[\text{MCl}_3(\text{EO}_3)]\cdot 18\text{-crown-6}$ ($\text{M} = \text{Dy}$, Y). A 10-mmol quantity of 18-crown-6 (containing triethylene glycol as an impurity) was added to a stirred solution of 10 mmol of $\text{MCl}_3\cdot 6\text{H}_2\text{O}$ ($\text{M} = \text{Dy}$ or Y) in 30 mL of $\text{CH}_3\text{OH}/\text{CH}_3\text{CN}$ (1:3) with excess LiCl present. The reaction mixture was heated to 60°C for 2.5 h; the supernatant was separated from the residual solid and then was cooled to 22°C . Crystallization took place over several days, with the formation of transparent parallelepiped crystals. Due to the "dirty" nature of this reaction and the impurities present, no analytical data were obtained. The crystalline material was studied during a period of low humidity, and no hygroscopic character was noted.

Synthesis and Crystallization of $[\text{M}(\text{OH}_2)_5(\text{EO}_3)]\text{Cl}_3$ ($\text{M} = \text{Nd}$, Eu , Gd , Dy , Y). A 3-mmol quantity of triethylene glycol (2.25 mmol for $\text{M} = \text{Nd}$, Eu) was added to a stirred solution of 3 mmol of $\text{MCl}_3\cdot 6\text{H}_2\text{O}$ ($\text{M} = \text{Nd}$ and Eu , 2.25 mmol) in 10 mL of $\text{CH}_3\text{OH}/\text{CH}_3\text{CN}$ (1:3). The reaction mixture was heated to 65°C for 2.5 h (60°C and 1 h for $\text{M} = \text{Nd}$, Eu), after which time a white powder was still present in the solution ($\text{M} = \text{Nd}$, clear purple solution; $\text{M} = \text{Eu}$, clear colorless solution). The mixture was centrifuged, the clear supernatant was decanted, and the solution was slowly cooled to 22°C .

For $\text{M} = \text{Nd}$ the volume was reduced by one-fourth, at which time a two-layer system formed. After 1 month the growth of small crystals

near the reaction vessel stopper was noted. The solution was placed under vacuum at -5°C , and immediately violet crystals formed. The crystals were stable to the moisture in air even during a period of high humidity. No solid formed in the $\text{M} = \text{Eu}$ reaction after cooling to -12°C . The volume was reduced by 10% under vacuum at -5°C and stored at -12°C . Crystallization began in 3 days, and suitable crystals had formed in 3 weeks.

Small, clear, square-shaped crystals formed within 2 h of cooling for $\text{M} = \text{Gd}$. Several days at room temperature were required for crystallization of $\text{M} = \text{Dy}$ and Y . $\text{M} = \text{Gd}$, Dy , and Y were stable to the moisture in air during periods of low humidity only. When $\text{M} = \text{Eu}$ was crystallized, the crystals were deliquescent during a period of high humidity.

Similar reactions were carried out with $\text{M} = \text{La}$, Ce , and Sm . Thus far each has formed the two-layer system observed for $\text{M} = \text{Nd}$, but suitable crystals for this study were not obtained. Analytical data have been obtained for twinned crystals of $\text{M} = \text{Sm}$ and are given below.

Each of the structurally characterized pentahydrates turns opaque at approximately 150°C and decomposes at $325\text{--}330^\circ\text{C}$. Analytical data were obtained for each. Anal. Calcd for $\text{M} = \text{Nd}$: C, 14.68; H, 4.93. Found: C, 14.55; H, 5.16. Calcd for $\text{M} = \text{Sm}$: C, 14.50; H, 4.87. Found: C, 14.34, H, 5.02. Calcd for $\text{M} = \text{Eu}$: C, 14.45; H, 4.85. Found: C, 13.86; H, 4.91. Calcd for $\text{M} = \text{Gd}$: C, 14.30; H, 4.80. Found: C, 14.45; H, 4.45. Calcd for $\text{M} = \text{Dy}$: C, 14.16; H, 4.75. Found: C, 13.95; H, 4.09. Calcd for $\text{M} = \text{Y}$: C, 16.55; H, 5.55. Found: C, 12.11; H, 4.84 ($\text{M} = \text{Y}$ appeared to suffer from hydrolysis in air).

Synthesis and Crystallization of $[\text{MCl}_3(\text{EO}_3)]\cdot \text{CH}_3\text{CN}$ ($\text{M} = \text{Ho}$, Lu). A 2.25-mmol quantity of the hexahydrated chloride salt was dissolved in 8.0 mL of $\text{CH}_3\text{OH}/\text{CH}_3\text{CN}$ (1:3). A 2.25-mmol amount of triethylene glycol was pipetted into the solution. The solution was heated with stirring to 60°C for 1 h. A powdered precipitate formed, peach for $\text{M} = \text{Ho}$ and white for $\text{M} = \text{Lu}$. The mixture was centrifuged hot, and the precipitate was washed twice with cold acetonitrile. The wet precipitate was covered and allowed to stand at 22°C . After 3 days the powders had become crystalline, small, pin-shaped, peach-colored crystals for $\text{M} = \text{Ho}$ and larger clear parallelepipeds for $\text{M} = \text{Lu}$. The crystals were deliquescent and dissolved when left exposed to air outside the solvent. The crystals were transferred to a drybox and inserted in capillary tubes. After several hours, crystals left out in the argon atmosphere of the drybox lost acetonitrile and became opaque and powdery. This deliquescent powder was analyzed as the anhydrous, solvent-free product.

Further analysis on the crystalline substances showed mp 305°C for $\text{M} = \text{Ho}$ and mp 325°C for $\text{M} = \text{Lu}$. Anal. Calcd for $\text{M} = \text{Ho}$ after loss of the solvent: C, 17.10; H, 3.35. Found: C, 16.07; H, 5.17. Calcd for $\text{M} = \text{Lu}$ after loss of the solvent: C, 16.70; H, 3.21. Found: C, 17.43; H, 3.57.

Synthesis and Crystallization of $[\text{MCl}_3(\text{EO}_3)]\cdot \text{OHMe}$ ($\text{M} = \text{Er}$, Yb). A 2.25-mmol quantity of $\text{ErCl}_3\cdot 6\text{H}_2\text{O}$ was dissolved in 7.0 mL of $\text{CH}_3\text{OH}/\text{CH}_3\text{CN}$ (1:3). A 2.25-mmol amount of triethylene glycol was pipetted into the solution. The solution was heated with stirring at 60°C for 1 h. The solution was allowed to cool slowly to 22°C and then cooled to -12°C and allowed to stand for 24 h. No solids formed. The solvent was reduced under vacuum by one-third. The solution was stored at -12°C until small pink crystals formed. ($\text{M} = \text{Lu}$ has also been isolated in a similar fashion and confirmed by preliminary unit cell determination.)

The analogous Yb complex was prepared in a similar fashion by starting with the anhydrous chloride. After it was heated for 1 h at 60°C , the mixture was centrifuged warm and the supernatant slowly cooled to 22°C . After several hours very large, clear, cubelike crystals (1.5 mm on edge) formed.

The crystals for both complexes were very deliquescent and were handled in an inert-atmosphere glovebox. The crystals were mounted in capillaries prior to X-ray examination. Unlike the CH_3CN adducts, which lose solvent readily, these crystals are stable to solvent loss when removed from solution under an inert atmosphere. Analytical data were obtained as follows for $[\text{MCl}_3(\text{EO}_3)]\cdot \text{OHMe}$. Anal. Calcd for $\text{M} = \text{Er}$: C, 18.45; H, 3.98. Found: C, 17.49; H, 4.03. Calcd for $\text{M} = \text{Yb}$: C, 18.21; H, 3.93. Found: C, 19.06; H, 4.50.

Synthesis and Crystallization of $[\text{LuCl}_3(\text{EO}_3)]$. The reaction of $\text{LuCl}_3\cdot 6\text{H}_2\text{O}$ with triethylene glycol as reported above was repeated in slightly less solvent (5.0 mL). Small colorless crystals formed overnight when the solution was cooled slowly from 60°C to 22°C . A crystallographic investigation of these crystals revealed there to be two different forms, the acetonitrile adduct above and the anhydrous, unsolvated product $[\text{LuCl}_3(\text{EO}_3)]$. Analytical data collected on these crystals were identical with those found previously and reported above.

X-ray Data Collection, Structure Determination, and Refinement. Transparent single crystals of the title complexes were either mounted

Table VII. Final Fractional Coordinates for $[\text{DyCl}_3(\text{EO}_3)]\cdot 18\text{-crown-6}$

atom	<i>x/a</i>	<i>y/b</i>	<i>z/c</i>	<i>U</i> (eqv) ^a
Dy	0.5000	0.78884 (3)	0.2500	0.017
Cl(1)	0.5000	0.5976 (2)	0.2500	0.022
Cl(2)	0.5977 (1)	0.8157 (1)	0.0828 (2)	0.039
O(1)	0.6113 (3)	0.7609 (3)	0.3745 (3)	0.026
O(2)	0.5623 (3)	0.9384 (3)	0.3275 (5)	0.039
O(3)	0.6895 (3)	0.5897 (3)	0.3905 (4)	0.028
O(4)	0.8198 (3)	0.6864 (3)	0.2873 (4)	0.031
O(5)	0.8526 (3)	0.8759 (3)	0.3877 (4)	0.030
C(1)	0.6457 (9)	0.844 (1)	0.445 (1)	(iso)
C(2)	0.5991 (8)	0.9298 (9)	0.440 (1)	(iso)
C(3)	0.5301 (8)	1.0304 (9)	0.270 (1)	(iso)
C(1)'	0.3374 (7)	0.8345 (9)	0.075 (1)	(iso)
C(2)'	0.368 (1)	0.928 (1)	0.103 (2)	(iso)
C(3)'	0.483 (1)	1.025 (1)	0.168 (2)	(iso)
C(4)	0.7306 (4)	0.5499 (5)	0.2966 (6)	0.034
C(5)	0.7586 (4)	0.6326 (5)	0.2250 (6)	0.033
C(6)	0.8453 (4)	0.7708 (5)	0.2268 (5)	0.031
C(7)	0.9007 (4)	0.8306 (5)	0.3051 (6)	0.033
C(8)	0.9020 (4)	0.9363 (5)	0.4611 (6)	0.035
C(9)	0.8475 (4)	0.9842 (5)	0.5424 (6)	0.036

^a*U*(eqv) is equal to (*U*₁₁ + *U*₂₂ + *U*₃₃)/3.

on pins or placed in capillary tubes and transferred to the goniometer. For studies at low temperature the crystals were cooled to -150 °C by using a stream of cold nitrogen gas. The space groups were determined from the systematic absences. For $[\text{MCl}_3(\text{EO}_3)]\cdot 18\text{-crown-6}$ and $[\text{M}(\text{OH}_2)_5(\text{EO}_3)]\text{Cl}_3$ centrosymmetric and noncentrosymmetric space groups were possible. The space group ultimately used reflects an investigation of both and subsequent successful solution and refinement. A summary of data collection parameters is given in Table VI for all structurally characterized complexes.

$[\text{MCl}_3(\text{EO}_3)]\cdot 18\text{-crown-6}$ (*M* = Dy, Y (20, -150 °C)). The dysprosium atom was located on a crystallographic 2-fold axis. Multiple sites for the ethylene units of the glycol molecule were evident early in the refinement. An investigation of the acentric space group *Cc* produced high correlations between the atoms related by the 2-fold axis and center of inversion and the continued presence of disorder. *C2/c* was retained and a disorder model developed involving two different conformations of the ethylene units. Because the C(3)-C(3)_a and C(3)'_a-C(3)'_a distances were not appropriate for a C-C single bond, the disorder was treated as 50% for each conformation C(1), C(2), C(3) and C(1)', C(2)', C(3)'. The thermal parameters for O(2) suggested fractional disorder, but it was not possible to resolve a disorder model. Due to the proximity of the disordered atoms the ethylene carbon atoms in the glycol molecule were refined isotropically and no attempt to locate or place hydrogen atoms around these groups was made. The crown ether hydrogen atoms and those of the glycol oxygen atom were located from a difference Fourier map and included with fixed contributions (*B* = 5.5 Å²). The two determinations of *M* = Y were treated in a similar manner. The positional parameters are given in Table VII for *M* = Dy; those for *M* = Y at 20 and -150 °C have been deposited in the supplementary material.

$[\text{M}(\text{OH}_2)_5(\text{EO}_3)]\text{Cl}_3$ (*M* = Nd, Eu, Gd, Dy, Y). The noncentrosymmetric space group *Pna2*₁ proved to be the correct choice for these complexes. Investigations of absolute configuration resulted in the *R* inverse values given in Table VI. *M* = Dy and Eu complexes have an absolute configuration opposite those of *M* = Nd, Gd, and Y complexes. The ethylene hydrogen atoms were placed in calculated positions 0.95 Å from the bonded carbon atoms and allowed to ride on that atom with *B* fixed at 5.5 Å². The remaining hydrogen atoms were not included in the final refinement. The positional parameters are given in Table VIII for *M* = Nd; those for *M* = Eu, Gd, Dy, and Y have been deposited in the supplementary material.

$[\text{MCl}_3(\text{EO}_3)]\cdot \text{CH}_3\text{CN}$ (*M* = Ho, Lu). The ethylene hydrogen atoms were treated as above. The hydrogen atoms bonded to the glycol oxygen atoms were located from a difference Fourier map and fixed (*B* = 5.5 Å²). Two of the acetonitrile hydrogen atoms were visible in a final difference Fourier; however, none of these atoms were included in the final refinement. The final positional parameters for *M* = Ho are given in Table IX; those for *M* = Lu have been deposited in the supplementary material.

$[\text{MCl}_3(\text{EO}_3)]\cdot \text{OHMe}$ (*M* = Er, Yb). The ethylene hydrogen atoms were treated as above. Two orientations with 50% occupancy each were noted for the methanol oxygen atom. These were refined in alternate cycles. The solvent hydrogen atoms and that for O(1) (hydrogen bonded to the disordered solvent) could not be located. Although the hydrogen

Table VIII. Final Fractional Coordinates for $[\text{Nd}(\text{OH}_2)_5(\text{EO}_3)]\text{Cl}_3$

atom	<i>x/a</i>	<i>y/b</i>	<i>z/c</i>	<i>U</i> (eqv) ^a
Nd	-0.29542 (3)	-1.01518 (4)	-0.2500	0.023
Cl(1)	-0.3342 (2)	-1.0131 (3)	0.1458 (3)	0.038
Cl(2)	-0.0680 (2)	-1.2628 (3)	-0.0497 (3)	0.038
Cl(3)	0.0290 (2)	-0.8537 (3)	-0.1350 (3)	0.032
O(1)	-0.1359 (4)	-0.9259 (8)	-0.2722 (6)	0.032
O(2)	-0.2467 (5)	-0.9699 (8)	-0.4429 (7)	0.026
O(3)	-0.3439 (5)	-1.1910 (7)	-0.3989 (6)	0.026
O(4)	-0.3987 (5)	-1.2026 (7)	-0.1906 (6)	0.031
O(5)	-0.2962 (4)	-0.7590 (7)	-0.254 (1)	0.034
O(6)	-0.4004 (5)	-0.9360 (8)	-0.0996 (6)	0.029
O(7)	-0.2151 (5)	-1.0316 (9)	-0.0697 (7)	0.037
O(8)	-0.4426 (5)	-0.9328 (8)	-0.3336 (7)	0.032
O(9)	-0.1904 (4)	-1.2206 (7)	-0.255 (1)	0.037
C(1)	-0.0937 (8)	-0.926 (1)	-0.380 (1)	0.041
C(2)	-0.1637 (8)	-0.886 (1)	-0.458 (1)	0.035
C(3)	-0.2602 (7)	-1.066 (1)	-0.5295 (9)	0.032
C(4)	-0.3442 (8)	-1.141 (1)	-0.5092 (9)	0.035
C(5)	-0.4219 (8)	-1.278 (1)	-0.3728 (9)	0.038
C(6)	-0.4095 (8)	-1.320 (1)	-0.259 (1)	0.038

^a*U*(eqv) is equal to (*U*₁₁ + *U*₂₂ + *U*₃₃)/3.

Table IX. Final Fractional Coordinates for $[\text{HoCl}_3(\text{EO}_3)]\cdot \text{CH}_3\text{CN}$

atom	<i>x/a</i>	<i>y/b</i>	<i>z/c</i>	<i>U</i> (eqv) ^a
Ho	0.11564 (3)	0.40366 (2)	0.35428 (1)	0.027
Cl(1)	-0.1476 (2)	0.3155 (2)	0.35499 (9)	0.047
Cl(2)	0.0377 (2)	0.4702 (1)	0.19676 (9)	0.045
Cl(3)	0.2411 (2)	0.3570 (2)	0.51188 (8)	0.042
O(1)	0.1520 (4)	0.2020 (4)	0.3163 (2)	0.044
O(2)	0.3613 (4)	0.3653 (4)	0.3292 (2)	0.040
O(3)	0.2806 (4)	0.5796 (4)	0.3731 (2)	0.038
O(4)	0.0037 (4)	0.5800 (4)	0.3926 (2)	0.042
C(1)	0.2825 (7)	0.1641 (7)	0.2859 (4)	0.059
C(2)	0.4126 (7)	0.2402 (6)	0.3352 (4)	0.059
C(3)	0.4803 (7)	0.4549 (6)	0.3562 (4)	0.054
C(4)	0.4073 (7)	0.5762 (6)	0.3341 (4)	0.052
C(5)	0.2078 (8)	0.6970 (6)	0.3668 (4)	0.047
C(6)	0.0927 (8)	0.6895 (6)	0.4188 (4)	0.049
N	0.483 (1)	0.4258 (9)	0.1245 (7)	0.138
C(7)	0.366 (1)	0.4535 (9)	0.0768 (7)	0.099
C(8)	0.225 (1)	0.4904 (9)	0.0241 (5)	0.078
H(1)[O(1)]	0.077	0.136	0.305	(iso)
H(1)[O(4)]	-0.087	0.586	0.420	(iso)

^a*U*(eqv) is equal to (*U*₁₁ + *U*₂₂ + *U*₃₃)/3.

Table X. Final Fractional Coordinates for $[\text{ErCl}_3(\text{EO}_3)]\cdot \text{OHMe}$

atom	<i>x/a</i>	<i>y/b</i>	<i>z/c</i>	<i>U</i> (eqv) ^a
Er	0.15239 (5)	0.41526 (2)	0.19258 (2)	0.025
Cl(1)	0.2737 (3)	0.5783 (1)	0.1685 (2)	0.043
Cl(2)	0.0529 (4)	0.4506 (2)	0.3528 (2)	0.060
Cl(3)	0.2280 (3)	0.3505 (1)	0.0334 (1)	0.039
O(1)	0.4536 (8)	0.3986 (3)	0.2742 (4)	0.040
O(2)	0.2227 (8)	0.2622 (3)	0.2519 (4)	0.036
O(3)	-0.1053 (8)	0.3104 (3)	0.1580 (4)	0.035
O(4)	-0.1098 (7)	0.4836 (3)	0.1016 (4)	0.035
C(1)	0.527 (1)	0.3100 (6)	0.3048 (7)	0.051
C(2)	0.379 (1)	0.2531 (6)	0.3329 (6)	0.045
C(3)	0.073 (1)	0.2020 (5)	0.2585 (6)	0.045
C(4)	-0.063 (1)	0.2132 (6)	0.1663 (7)	0.055
C(5)	-0.243 (1)	0.3324 (5)	0.0746 (6)	0.041
C(6)	-0.285 (1)	0.4348 (6)	0.0855 (6)	0.045
O(5)	0.675 (2)	0.5319 (8)	0.3407 (9)	0.049
O(5)'	0.658 (2)	0.506 (1)	0.391 (1)	0.079
C(7)	0.613 (2)	0.5916 (7)	0.4140 (8)	0.073

^a*U*(eqv) is equal to (*U*₁₁ + *U*₂₂ + *U*₃₃)/3.

atom bonded to O(4) was clearly visible in a difference Fourier, it was not included in the final refinement. The final positional parameters for *M* = Er are given in Table X; those for *M* = Yb have been deposited in the supplementary material.

$[\text{LuCl}_3(\text{EO}_3)]\cdot \text{CH}_3\text{CN}$. This complex was isolated from the same reaction that gave $[\text{LuCl}_3(\text{EO}_3)]\cdot \text{CH}_3\text{CN}$. Data were collected at -150 °C. The space group, *Pbcn*, was uniquely determined from the systematic absences. All hydrogen atoms were included with fixed contributions (*B*

Table XI. Final Fractional Coordinates for [LuCl₃(EO₃)]

atom	<i>x/a</i>	<i>y/b</i>	<i>z/c</i>	<i>U</i> (eqv) ^a
Lu	0.5000	-0.07703 (3)	0.2500	0.006
Cl(1)	0.5000	0.0950 (2)	0.2500	0.014
Cl(2)	0.7499 (2)	-0.0981 (1)	0.4051 (1)	0.013
O(1)	0.3012 (6)	-0.0459 (3)	0.3978 (5)	0.014
O(2)	0.3847 (6)	-0.2088 (4)	0.3379 (4)	0.011
C(1)	0.226 (1)	-0.1187 (5)	0.4718 (7)	(iso)
C(2)	0.2118 (9)	-0.1982 (5)	0.3917 (7)	0.011
C(3)	0.408 (1)	-0.2942 (5)	0.2723 (7)	0.016
H(1)[O(1)]	0.321	-0.004	0.440	(iso)

^a*U*(eqv) is equal to (*U*₁₁ + *U*₂₂ + *U*₃₃)/3.

= 5.5 Å²) in the final refinement. C(1) could not be refined anisotropically. The final positional parameters are given in Table XI.

Acknowledgment. We wish to thank the Illinois Department of Commerce and Community Affairs and the donors of the Petroleum Research Fund, administered by the American

Chemical Society, for support of this work. The U.S. National Science Foundation's Chemical Instrumentation Program provided funds used to purchase the diffractometer.

Registry No. [DyCl₃(EO₃)]·18-crown-6, 111976-41-1; [YCl₃(EO₃)]·18-crown-6, 111976-39-7; [Nd(OH₂)₅(EO₃)]Cl₃, 111976-45-5; [Eu(OH₂)₅(EO₃)]Cl₃, 111976-44-4; [Gd(OH₂)₅(EO₃)]Cl₃, 111976-43-3; [Dy(OH₂)₅(EO₃)]Cl₃, 111997-42-3; [Y(OH₂)₅(EO₃)]Cl₃, 111976-42-2; [HoCl₃(EO₃)]·CH₃CN, 111976-37-5; [LuCl₃(EO₃)]·CH₃CN, 111976-35-3; [ErCl₃(EO₃)]·OHMe, 111976-34-2; [YbCl₃(EO₃)]·OHMe, 111976-32-0; [LuCl₃(EO₃)]₂, 111976-30-8; [Sm(OH₂)₅(EO₃)]Cl₃, 111976-46-6.

Supplementary Material Available: Tables SI-SXLI, listing hydrogen atom coordinates and thermal parameters for all complexes, fractional coordinates for those complexes not in the text, hydrogen bond contact geometries, bond distances and angles for the 18-crown-6 complexes, and representative least-squares plane results (27 pages); Tables SXLII-SLIV, listing observed and calculated structure factors or structure factor amplitudes for all complexes (93 pages). Ordering information is given on any current masthead page.

Contribution from the Laboratoire de Spectrochimie des Eléments de Transition, UA No. 420, and Laboratoire de Chimie Physique des Matériaux Amorphes, UA No. 1104, Université de Paris Sud, 91405 Orsay, France, Department of Chemistry, University of Bergen, 5007 Bergen, Norway, and Departamento de Química Inorgánica, Facultad de Ciencias Químicas, Burjassot, Valencia, Spain

Phase Transition and Exchange Interaction in (μ-Carbonato)bis[(*N,N,N',N'',N'''*-pentaethyldiethylenetriamine)copper(II)] Diperchlorate

Jorunn Sletten,^{*1a} Hakon Hope,^{1a,c} Miguel Julve,^{1b} Olivier Kahn,^{*1c} Michel Verdager,^{1c}
and Ary Dworkin^{1d}

Received August 6, 1987

The title compound, [(Cu(petdien))₂(CO₃)](ClO₄)₂, has been synthesized and its crystal structure has been determined at 294 K (high-temperature (HT) modification) and 92 K (low-temperature (LT) modification). Crystal data: for HT, orthorhombic system, space group *Cmc*2₁, *a* = 18.610 (3) Å, *b* = 15.449 (3) Å, *c* = 14.499 (7) Å, *Z* = 4; for LT, monoclinic system, space group *P*2₁, *a* = 12.037 (1) Å, *b* = 13.145 (3) Å, *c* = 12.519 (2) Å, β = 96.85 (1)°, *Z* = 2. The phase transition between the HT and the LT forms occurs around 208 K. For the two modifications, the structure consists of dinuclear cations and noncoordinated perchlorate ions. Copper(II) is located in distorted-trigonal-bipyramid surroundings. An oxygen atom of the carbonato bridge is bound to the two copper atoms of the dinuclear unit; each of the other two oxygen atoms is bound to only one copper atom. In the LT modification, the Cu-O distances involving the doubly coordinated oxygen atom are in average 0.06 Å shorter than in the HT modification, but the average of the metal-ligand bond lengths remains unchanged. The magnetic properties have been investigated in the 300-20 K temperature range. The molar magnetic susceptibility exhibits a break at *T*_c, with an hysteresis of about 3 K. The S-T energy gap has been found to be *J* = -207 (1) cm⁻¹ above *T*_c and *J* = -215 (1) cm⁻¹ below *T*_c. The enthalpy and entropy variations associated with the phase transition have been determined by differential scanning calorimetry measurements and found to be Δ*H* = 3.17 (4) kJ mol⁻¹ and Δ*S* = 15.1 (2) J mol⁻¹ K⁻¹.

Introduction

In several cases, a temperature dependence of the exchange parameter *J* in an exchange-coupled system has been postulated or even demonstrated.²⁻⁵ The most likely origin of this phenomenon is a change of the geometrical structure of the system versus the temperature. This change may be gradual, without phase transition, or abrupt. In this latter case, it is associated with a crystallographic phase transition. A gradual change may occur when the bridging network has a specific nonrigidity. One of us called this phenomenon the exchange elasticity and reported such a situation in copper(II) dinuclear compounds resulting from the inclusion of the two metallic sites into intramolecular cavities containing two cation binding subunits.⁴ Another convincing

example of exchange elasticity due to the flexibility of the bridges is provided by hydrogen-bonded copper dimers.²

The solid-state physicists have often described small deviations of the magnetic properties from the predictions of the Heisenberg spin Hamiltonian in terms of exchange striction.⁶⁻⁸ Basically, the exchange striction results from a modulation of *J* due to the molecular vibrations. A nice example of temperature dependence of *J* in a Cr(III) dinuclear complex, attributed to exchange striction, has been given by Güdel and Furrer.³ The relative energies of the low-lying states in that case have been accurately determined by inelastic neutron scattering. A temperature dependence of *J* could also arise from the fact that the vibrational levels associated with a given low-lying electronic state depend on this state.⁹

To be complete, it is fair to say that in some works to which we will not refer, the claimed temperature dependence of *J* has its origin in the uncertainties of the experimental data. Such an

(1) (a) University of Bergen. (b) Facultad de Ciencias Químicas Valencia. (c) UA No. 420, Université de Paris Sud. (d) UA No. 1104, Université de Paris Sud. (e) On leave from the University of California, Davis, CA 95616.

(2) Duggan, D. M.; Hendrickson, D. N. *Inorg. Chem.* 1974, 13, 2929.

(3) Güdel, H. U.; Furrer, A. *Mol. Phys.* 1977, 33, 1335.

(4) Kahn, O.; Morgenstern-Badarau, I.; Audière, J. P.; Lehn, J. M.; Sullivan, S. A. *J. Am. Chem. Soc.* 1980, 102, 5935.

(5) Mikuriya, M.; Okawa, H.; Kida, S. *Bull. Chem. Soc. Jpn.* 1981, 54, 2979.

(6) Kennedy, T. A.; Choh, S. H.; Seidel, G. *Phys. Rev. B: Solid State* 1970, 2, 3645.

(7) Lines, M. E. *Solid State Commun.* 1972, 11, 1615.

(8) Katriel, J.; Kahn, O. *Phys. Lett. A* 1976, 55A, 439.

(9) Martin, R. L. *Inorg. Chem.* 1966, 5, 2065.